

Electric maneuvering of a side hinged ramp cover

Examensarbete för maskiningenjörsprogrammet

SANDRA JOHNSON
VALDEMAR KERPENS

Institutionen för Produkt- och produktionsutveckling
CHALMERS TEKNISKA HÖGSKOLA
Göteborg, Sverige 2014

Electric maneuvering of a side hinged ramp cover

SANDRA JOHNSON
VALDEMAR KERPENS

**Institutionen för Produkt- och produktionsutveckling
CHALMERS TEKNISKA HÖGSKOLA
Göteborg, Sverige 2014**

Electric maneuvering of a side hinged ramp cover
SANDRA JOHNSON
VALDEMAR KERPENS

© SANDRA JOHNSON, VALDEMAR KERPENS, 2014

Institutionen för Produkt- och produktionsutveckling
Chalmers tekniska högskola
SE-412 96 Göteborg
Sverige
Telefon: + 46 (0)31-772 1000

Preface

This bachelor thesis is performed at TTS Marine AB, a company focusing on transportation solutions for the marine industry.

This thesis include 15 university credits and was done during the spring semester in 2014 and was the final part of the mechanical engineering education (180 credits) at Chalmers University of Technology in Gothenburg.

We, Sandra Johnsson and Valdemar Kerpens, would like to take the opportunity and thank all the personnel at TTS Marine office in Gothenburg. Special thanks to our mentors, Peter Adolphsson and Henrik Westermark, at TTS for all your support. We also want to thank our mentor at Chalmers, Kjell Melkersson, for your help during our last semester and Peter Rydh from PMC Swedrive for the technical support.

Sammanfattning

TTS Marine AB är ett dotterbolag till TTS Group ASA som har som sitt huvudsakliga affärsområde inom den marina industrin. Kundens intresse för elektriska lösningar kontra hydrauliklösningar har ökat eftersom det traditionella hydrauliska systemet har en läckagerisk samt en negativ miljöpåverkan om det kommer i havet. En produkt som i dag drivs av hydrauliska cylindrar är TTS sidohängslade rampluckor. De fungerar som extra lastutrymme då luckan efter stängning och låsning kan lastas ovanpå. Projektet har fokuserats på att skapa en lösning för att göra lyftsystemet elektriskt istället för hydrauliskt. En avgränsning som gjorts var att inte förändra luckans geometri.

Det valda konceptet, Screw jack with push rod, är baserat på en lyftstång som är ansluten till en vagn med glidklossar. Denna vagn kommer att glida längs ett spår som kommer att svetsas till undersidan av rampluckan. En motor och en skruvdomkraft kommer att kunna dra och skjuta vagnen i spåret mot respektive från luckans gångjärn t.ex. då vagnen glider utmed spåret mot luckans gångjärn kommer lyftstången att pressa upp luckan.

Den framtagna lyftmekanismen är lika bra och funktionell som den befintliga, utan att vara mer komplicerad att installera och använda. Lösningen möjliggör även samma fria utrymme under luckan som den befintliga, så att den önskade lasten kan stuvvas precis som i dag.

Abstract

TTS Marine is a subsidiary of TTS Group ASA which has the marine industry as its main business area. The customers' interest for non-hydraulic solutions versus hydraulic solutions has increased since the hydraulic system has a leakage risk and a negative effect on the environment were it to leak and reach the ocean. One product that is today driven by hydraulic cylinders is TTS' side hinged ramp covers. They serve as extra loading area since after closing and locking the cover, cargo can be loaded on it. This project focuses on creating a solution to make the lifting system electric instead of hydraulic. One of the delimitations imposed by TTS is not to alter the geometry of the ramp cover.

The chosen concept, Screw jack with push rod, is based on a lifting rod connected to a wagon with glide pads. This wagon will slide along a track that will be welded to the underside of the ramp cover. A motor and a screw jack will pull and push the wagon in the track against respectively away from the ramp cover's hinge for example when the wagon slides along the track against the ramp cover's hinge a rod will push the ramp cover open.

The developed lifting mechanism is as good and functional as the existing, without making it more complicated to install or use. It also delivers the same free space under the ramp cover as the existing so that the desired cargo can be stowed in just like it did before.

Table of contents

1 Introduction	1
1.1 About TTS Marine AB.....	1
1.2 Purpose	1
1.3 Side hinged ramp cover.....	1
1.4 Requirements list.....	3
1.5 Delimitations	3
1.6 Delineation of the problem.....	3
2 Method	4
2.1 Preliminary study	4
2.2 Analysis of the current design	4
2.3 Brainstorming.....	4
2.4 Sorting the concepts	4
2.5 Feasibility analysis of the best concepts.....	4
2.6 Thorough analysis of the winning concept	4
2.7 Comparison with the current design.....	4
3 Reference frame	5
3.1 Neglection of the angular acceleration.....	5
3.2 Friction	6
3.3 Area moment of inertia in buckling	6
3.4 Screw jack	7
3.5 Mechanical cylinder	8
4 Existing design	9
5 The chosen concept	11
5.1 Screw jack with push rod	11
5.1.1 Screw jack	13
5.1.2 Wagon	15
5.1.3 Push rod.....	15
5.1.4 Guide track	16
5.2 Cost review.....	17
6 Discussion	18
7 Conclusions	19
References	20
<i>Appendix A. Existing Design.....</i>	<i>A1</i>
<i>Appendix B. Screw jack with push rod – the final concept</i>	<i>B1</i>

<i>Appendix C. Concepts analyzed further</i>	C1
<i>Appendix D. Economic references</i>	D1
<i>Appendix E. The rejected solutions</i>	E1

1 Introduction

1.1 About TTS Marine AB

TTS Marine AB is a subsidiary of TTS Group ASA which has the marine industry as its main business area. TTS Marine AB is part of the TTS Marine division with its focus within Cargo Access Equipment, such as ramps for internal and external use, ramp covers, movable car decks etc.

1.2 Purpose

TTS' customers' interest for electric solutions versus hydraulic solutions has increased since the hydraulic system has a leakage risk and a negative effect on the environment were it to leak and reach the ocean. TTS has developed electric solutions for most of its products. One product missing a cost effective electric operation system and is today driven by hydraulic cylinders is the side hinged ramp cover. This project focuses on creating a solution to make the lifting system electric instead of hydraulic.

1.3 Side hinged ramp cover

TTS' side hinged ramp covers are used to cover a fixed ramp and serve as extra loading area since after closing and locking the cover, cargo can be loaded on it. The cover is also used as a safety feature, in case a lower deck should become flooded the cover will prevent further flooding of the decks above.

In Figure 1.1 below a side view representation of a fixed ramp and its ramp covers can be seen, on the lower right corner of the figure is a schematic picture of where the ramp will be fitted in the ship. The panel 1 (ramp cover 1) is open so cargo can be placed in the lower deck, this is also illustrated in Figure 1.2.

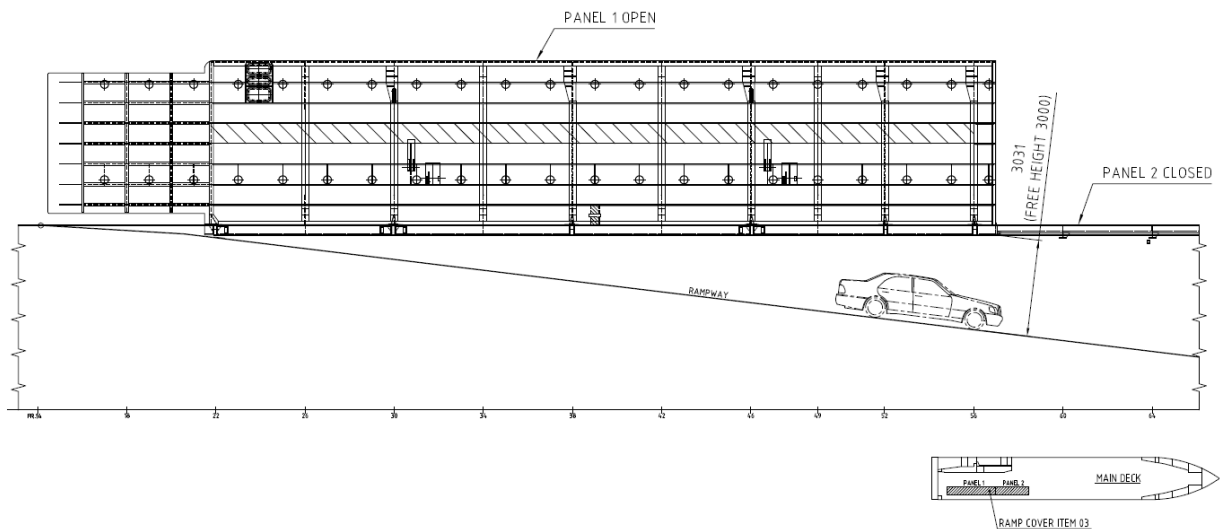


Figure 1.1: Side view of a ramp and its two ramp covers (panels)

The ramp cover is conventionally operated by a pair of hydraulic cylinders, see Figure 1.2 below.



Figure 1.2: Side hinged ramp cover operated by two hydraulic cylinders

Hydraulic cylinders are a well-established solution due to their high load-lifting capabilities. However, the disadvantage when using hydraulics is the leakage risk [1]* which could damage the cargo and/or surrounding environment. The plumbing, hereinafter referred to as piping, required to feed these hydraulic cylinders with oil is costly, time consuming and hard to install to a satisfactory quality within the ship/ramp steel structure [2].

The drawbacks presented above are the main reason why TTS is developing their product line to include a non-hydraulic solution to operate these ramp covers.

In Figure 1.3 a side hinged ramp cover is illustrated. The cylinders used in this type of design are of double acting type, which means they can be used for both pushing and pulling.

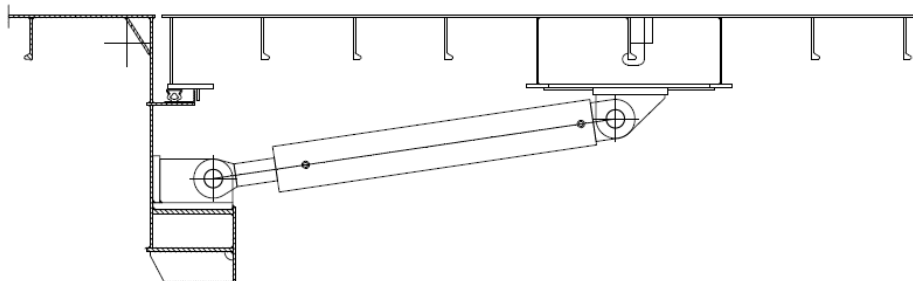


Figure 1.3: Side view drawing of a side hinged ramp cover (A40705)

*Number in square brackets [] designate references

1.4 Requirements list

TTS has some requirements for the electric driven lifting system of the side hinged ramp cover. The product has to be as good and functional as the existing, without making it more complicated to install or use. The new solution has to deliver the same free space as the existing so that the desired cargo can fit in just like it did before. Based on these conditions the following list has been made:

- **Opening time**
The opening operation should take about one minute.
- **Integration**
The lifting mechanism has to be built-in the ramp cover as much as possible since TTS has total control over the ramp cover design but not over the area around the ramp cover.
- **Space**
Requirements for headroom under the ramp cover, the same space as with the current design.
- **Cargo interference**
Nothing is allowed to stick outside the ramp cover when it's opened, it would disturb the loading operation.
- **Complexity**
Has to be simple in order to minimize the number of error factors and to be quick and easy to design and install.
- **Cost efficiency**
Equivalent to the current hydraulic design
- **Self-locking**
The ramp cover isn't allowed to sink during a stop in the maneuvering.

1.5 Delimitations

This report has the following delimitations:

- Only the lifting mechanism of the side hinged ramp covers is taken into account.
- No change in the geometry of the ramp cover.
- No consideration of the cleating system.

When comparing the cost between the established system and the new solution no account will be taken to the cost of the hydraulic pump station, because this pump will be serving several other hydraulic systems as well and will therefore be needed anyway.

1.6 Delineation of the problem

Can a non-hydraulic solution produce the same results as a hydraulic system without compromising its function?

Will the opening and closing procedure retain the same simplicity?

Will the new solution be cost effective and be able to compete with the cost of the hydraulic system?

2 Method

The used method can be divided into the following subcategories below.

2.1 Preliminary study

A survey of the existing design was done by looking through the data about the side hinged ramp covers. This was done by inventorying all the existing drawings and making a list of all the covers, their dimensions, mass and what kind of cylinders that were being used. By doing this list and by inventorying all the existing designs a better understanding of the function of the side hinged ramp covers was obtained.

2.2 Analysis of the current design

Calculations of the required lifting force were performed and the different covers existing today were analyzed. This in order to get the most common designs and their dimensions. By looking at all these parameters a complete understanding was obtained about what kind of forces the product must withstand.

2.3 Brainstorming

During the brainstorming there came up some different solutions how to make the side hinged ramp cover without a hydraulic system. This brainstorming was done with some of the people at the TTS office; Henrik Westermarck (R&D Manager), Peter Adolphsson (R&D Designer), Mauri Lehtonen (Senior Design Engineer), Ola Wallin (Project Manager) and Torbjörn Persson (Senior Design Engineer). All the solutions that came up were documented and can be found and described in Appendix B, Appendix C and Appendix E.

2.4 Sorting the concepts

The sorting process was done in junction with TTS personnel and consisted of checking which concepts where feasible both technically and economically. The requirements list was a crucial reference in the sorting process.

2.5 Feasibility analysis of the best concepts

Perform a thorough analysis of the best concepts: calculate the forces required to operate the system and estimate the costs involved in each concept.

2.6 Thorough analysis of the winning concept

This analysis consisted of modelling the concept in AutoDesk Inventor, and then perform a dynamic simulation, which showed the forces in the mechanism during the opening operation and finally a FE-analysis which helped to decide the mechanism's geometry.

2.7 Comparison with the current design

The current design was used as a benchmark, all the calculations, positive and negatives aspects of the concepts generated during the brainstorming were compared with the current design. This was done to ensure that the new concept would be as good as the current design.

3 Reference frame

When designing the new lifting concept of the ramp cover a representative ramp cover by TTS Marine AB was used (A40705). This because there is a wide range of ramp covers with different dimensions. With this in mind, all equations were kept as generalized as possible. These equations can be found throughout the appendices.

3.1 Neglection of the angular acceleration

When the different forces required for opening the ramp cover were calculated, the angular momentum was used. However, the angular acceleration is so small that it becomes negligible, proven below, and was therefore ignored. The angular momentum was transformed to a general equilibrium problem, and this type of equation was used consequently through all calculations of forces.

The angular momentum law:

$$\sum M_y = I_y \cdot \ddot{\theta} \Rightarrow F_{lift} \cdot q - mgx = I_y \cdot \ddot{\theta} \quad \text{Equation A.1}$$

- The index y describes the axis that goes right through the axis of the ramp cover's hinge
- I_y is the mass inertia around the y axis
- $\ddot{\theta}$ is the angular acceleration of the opening angle which means the angle between the ramp cover and the deck.
- F_{lift} = the lifting force from the rod
- q = the perpendicular distance between the ramp cover's hinge and the rod (the lever for force F_{lift})
- m = mass of ramp cover 10155 kg
- x = distance from the hinge to the center of mass 2,325 m
- g = the gravitational acceleration 9,81 m/s²

The angular acceleration $\ddot{\theta}$ and the inertia I_y used below were obtained by modeling a ramp cover in Inventor and running a dynamic simulation. The Figure 3.1 shows a cross section of the ramp cover modeled, with $m = 10155$ kg and $x = 2,325$ m.

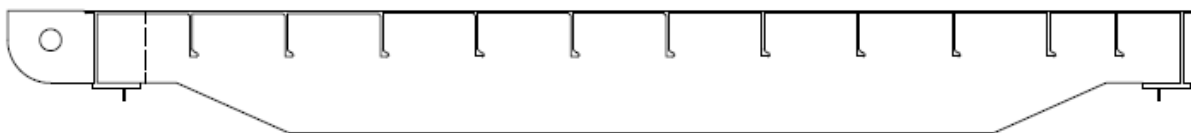


Figure 3.1: A cross section view of the ramp cover A40705

The result became:

$$I_y = 21200 \text{ kgm}^2$$

$$\ddot{\theta} = 0,001397 \text{ rad/s}^2$$

These values inserted in Equation A.1 gives:

$$F_{lift} \cdot q = mgx + I_y \cdot \ddot{\theta} \approx 12500 \cdot 9,81 \cdot 2,325 + 29,6 \approx 285103 + 29,6 \text{ [Nm]}$$

The contribution from the gravity gives a much higher momentum than the momentum caused by the product of the angular momentum and the inertia, making the factor $I_y \cdot \ddot{\theta}$ negligible.

3.2 Friction

There are energy losses due to friction in all the concepts described in the report, but limited consideration has been taken to any type of friction in either one of the concepts since it was outside of the scope of this analysis.

In the chosen concept friction is involved in all the mechanical parts such as: axles, gears, the connection between the spindle and the traveling nut and the interface between the guide pads and the guide track. These losses were also not taken into account, with the exception of the guide pads and the guide track, see Appendix B.

3.3 Area moment of inertia in buckling

In the concepts that came up from the brainstorming there are some components that will have to withstand compression forces. When analyzing a beam that was exposed to buckling the cross section geometry that was used was a hollow rectangle. The reason for this is that a hollow rectangular cross section has higher area moment of inertia against bending than a circular cross section with the same surface area.

The area of a hollow rectangle is $A_{rectangle} = W \cdot H - w \cdot h$ where W is width of the rectangle and H is its height, w is the width of the rectangular hole and h is its height.

Suppose that:

$$W = H = 120 \text{ [mm]} \text{ and } w = h = 86 \text{ mm } A_{rectangle} = 120^2 - 86^2 = 7004 \text{ mm}^2$$

If the circular beam has the same amount of material as the rectangular one, that means if the circular cross section has the same area as the rectangular one, then:

$$A_{circular} = \frac{\pi \cdot D^2}{4} = A_{rectangle} \Leftrightarrow D = \sqrt{\frac{7004}{\pi}} \approx 94,4 \text{ mm}$$

$$I_{rectangle} = \frac{W \cdot H^3}{12} - \frac{w \cdot h^3}{12} \approx 12,72 \cdot 10^6 \text{ mm}^4$$

$$I_{circular} = \frac{\pi \cdot D^4}{64} \approx 3,898 \cdot 10^6 \text{ mm}^4$$

As seen above, the area moment of inertia [3] is superior with the rectangular cross section than with circular cross section when they are made of the same amount of material.

If the cross section is instead a circle with a hole in it, and it uses the same amount of material as the rectangular cross section then there is an infinite amount of solutions to the following equation: $A_{circle\ w/\ hole} = \pi R^2 - \pi r^2 = A_{rectangle}$ where R and r are the radii of the circle and its hole. That is because R can be anything. But if the cross section has to have identical dimensions as the rectangular cross section and use the same amount of material and R is

$$\text{assumed to be } 60 \text{ mm} \Rightarrow r = \sqrt{\frac{\pi 60^2 - 7004}{\pi}} = 37 \text{ mm}$$

$$I_{circle\ w/hole} = \frac{\pi}{64}(D^4 - d^4) \approx 8,7 \cdot 10^6\ mm^4$$

Even here, the rectangular cross section has a higher area moment of inertia.

3.4 Screw jack

A screw is driven by electric power and consists of a motor, a worm gear, a spindle and a traveling nut, see Figure 3.2. There are two main variants of screw jacks: one where the screw (spindle) rotates around its longitudinal axle and the other where the spindle translates through the gears. The later won't be taken into consideration in this report.

A screw jack is very similar to a mechanical cylinder but instead of having a traveling nut connected to a telescopic rod that covers the screw (spindle), see Figure 3.3, the traveling nut is attached to the structure that will be lifted, see Figure 3.2. This traveling nut can be equipped with holes in order to be bolted to the lifted structure. The fastening of the traveling nut is crucial, since without the fastening it would rotate as it travels along the spindle. The screw jack transforms rotational movement from the motor to a translational movement of the traveling nut.

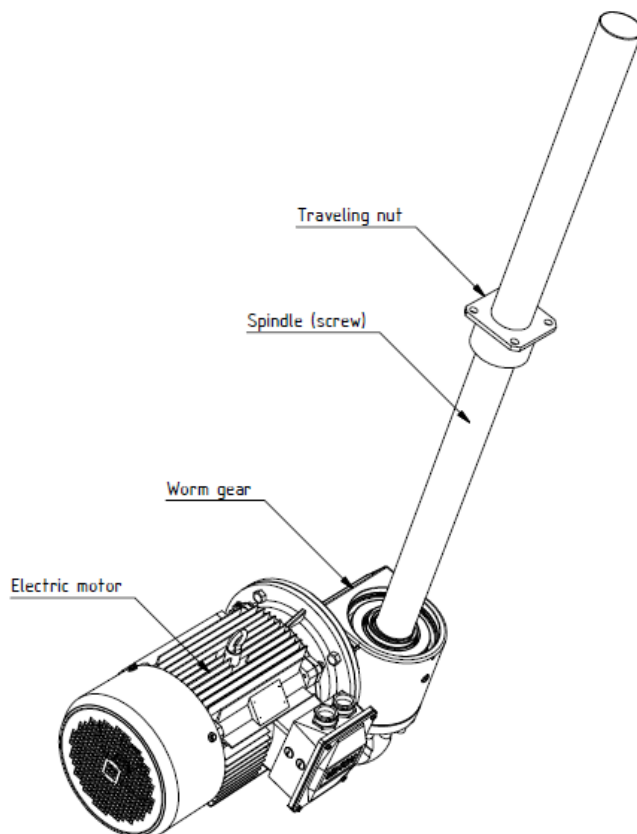


Figure 3.2: Screw jack with a traveling nut [4]

3.5 Mechanical cylinder

Throughout the report the component called mechanical cylinder is mentioned. A mechanical cylinder is very similar to a screw jack but its traveling nut is connected to a telescopic rod. At the end of the telescopic rod there is an ear, used to fixate the mechanical cylinder to a structure, see Figure 3.3. A mechanical cylinder is generally sold as a unit. To summarize, a mechanical cylinder is a linear transmission that has the same function as a hydraulic cylinder.



Figure 3.3: Mechanical cylinder [4]

Screw jacks and mechanical cylinders can often be used in the same kind of applications, although the cost of a mechanical cylinder is slightly higher.

4 Existing design

By investigating TTS's reference product archive the following information could be gathered:

- Mass and dimensions of TTS' side hinged ramp covers
- Required lifting force to maneuver such ramp covers
- Most common size of the hydraulic cylinders used in hinged ramp covers

Figure 4.1, shows a typical cylinder lifting the side hinged ramp cover.

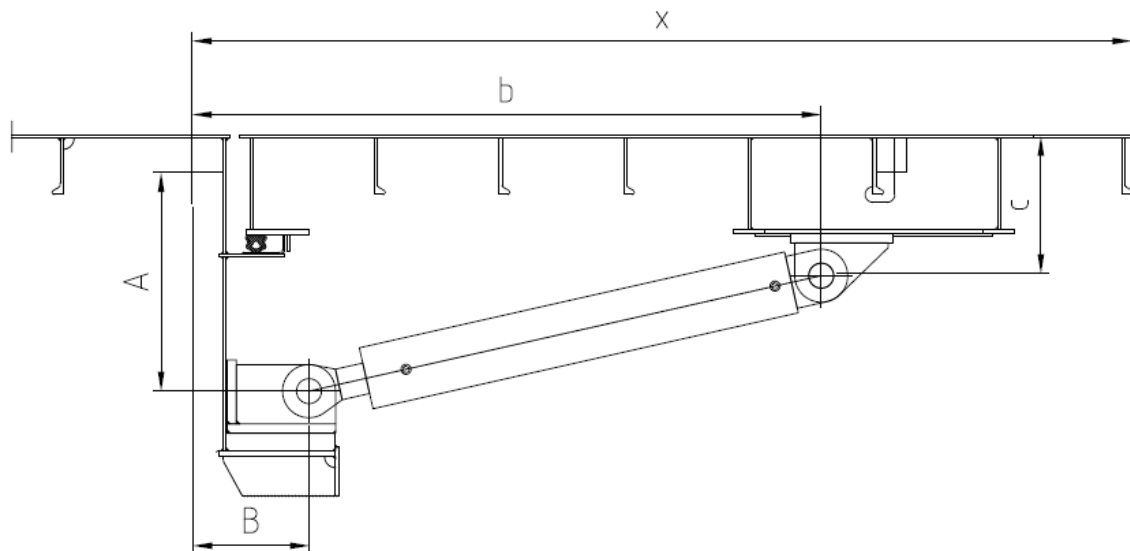


Figure 4.1: Drawing of a side hinged ramp cover (article no. A40705)

Figure 4.1 also illustrates the input parameters for the diagram below. The calculations used to draw the diagram in Figure 4.2 can be found in Appendix A. The diagram shows the lifting force as a function of the opening angle. The angle varied between 0 to 90 degrees. The side hinged ramp cover used for the input parameters has the article number A40705.

Inputs:

$$c = 0,33 \text{ m}$$

$$x = 2,3175 \text{ m}$$

$$A = 0,7 \text{ m}$$

$$B = 0,375 \text{ m}$$

$$b = 2,019 \text{ m}$$

$$\text{Mass of ramp cover } m = 20301 \text{ kg}$$

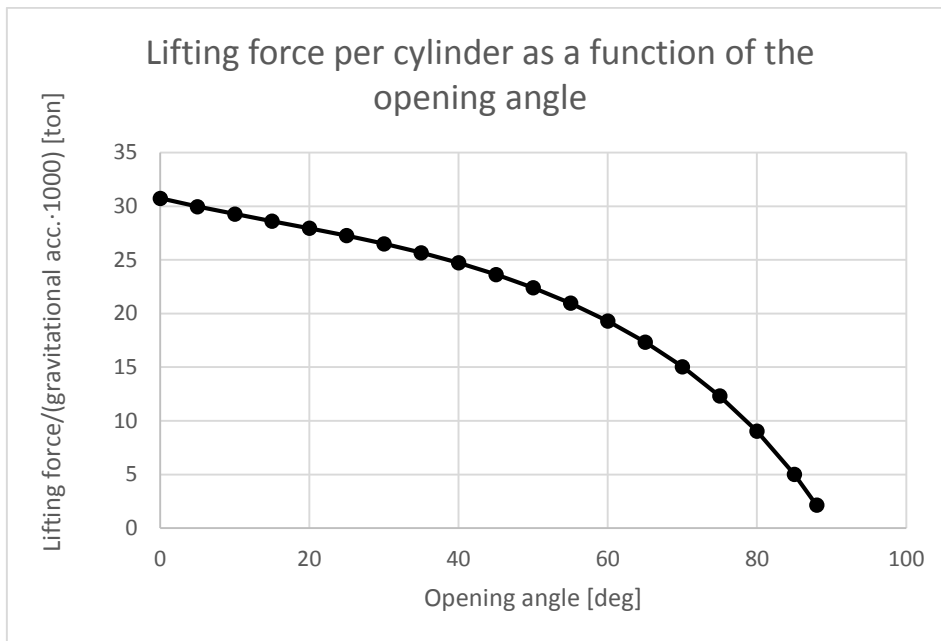


Figure 4.2: Diagram of the lifting force as a function of the opening angle

5 The chosen concept

The concept Screw jack with push rod was chosen because of its simplicity in comparison to the other concepts analyzed and its cost was equivalent to the current hydraulic design.

5.1 Screw jack with push rod

In this concept the mechanism is located under the ramp cover and it follows the ramp cover during the entire operation. It uses a push rod with constant length to push the ramp cover open. The push rod is connected to a wagon that translates in a guide track fixed to the longitudinal beams of the cover, see Figure 5.1. The wagon will be pulled down the track towards the cover's hinge by a traveling nut that is threaded on a rotating spindle, see also Figure 5.2 and Figure 5.3. To avoid buckling in the spindle, since it would become expensive to dimension it against buckling, the sliding push rod is used. Here the rod will have to withstand buckling instead of the spindle, since it's more cost efficient to dimension the rod against buckling. During the initial instants of the closing operation the screw jack will push the wagon in the opposite direction, away from the hinge. Since the traveling nut at this instant is close to the bearing that fixates the spindle axially, the spindle will not buckle during the operation due to the rather short effective column length [6].

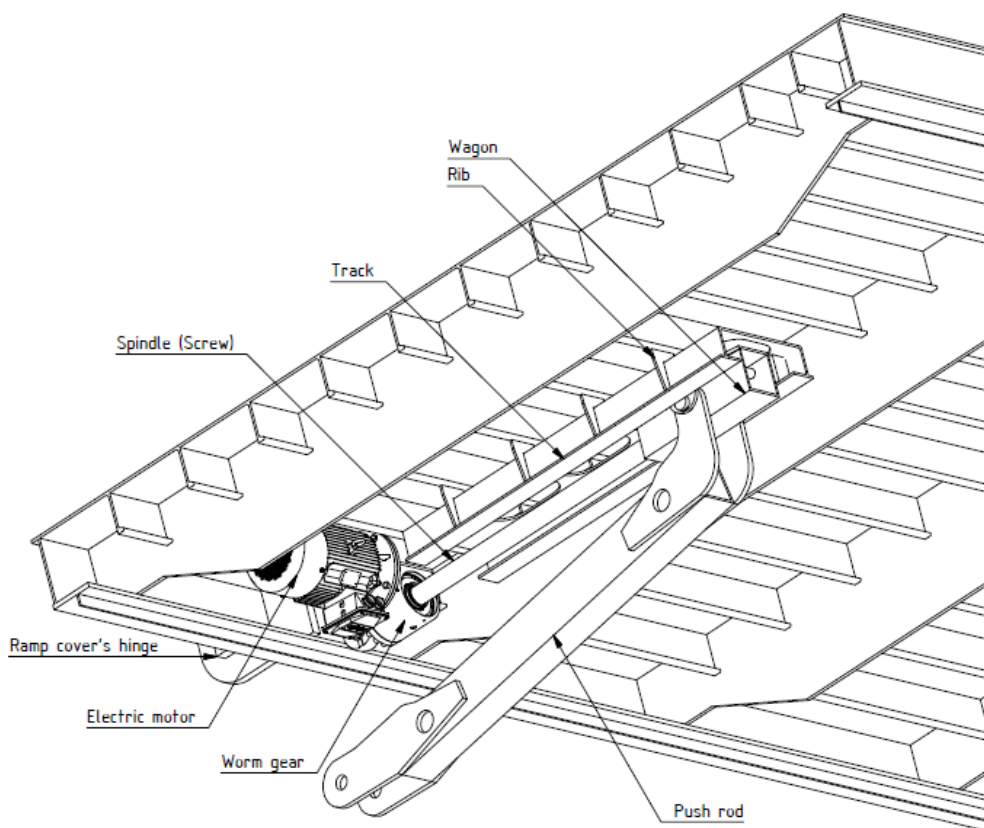


Figure 5.1: Screw jack with push rod

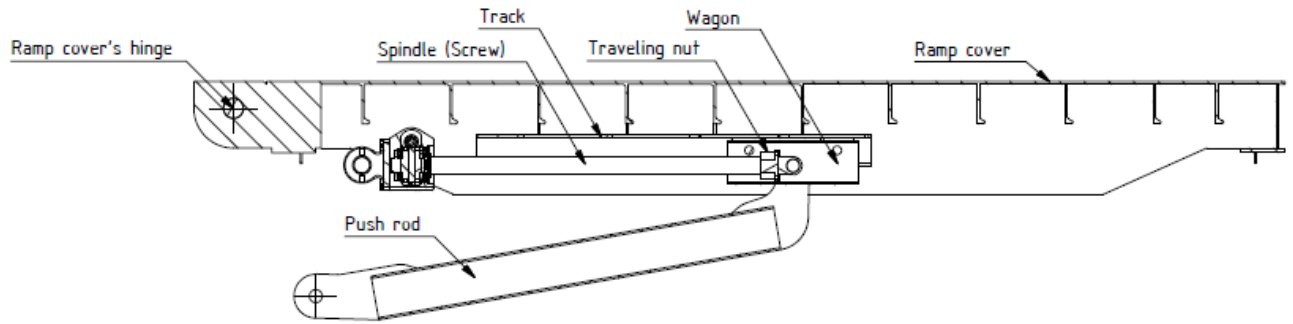


Figure 5.2: A cross section view of the final concept while the ramp cover is closed

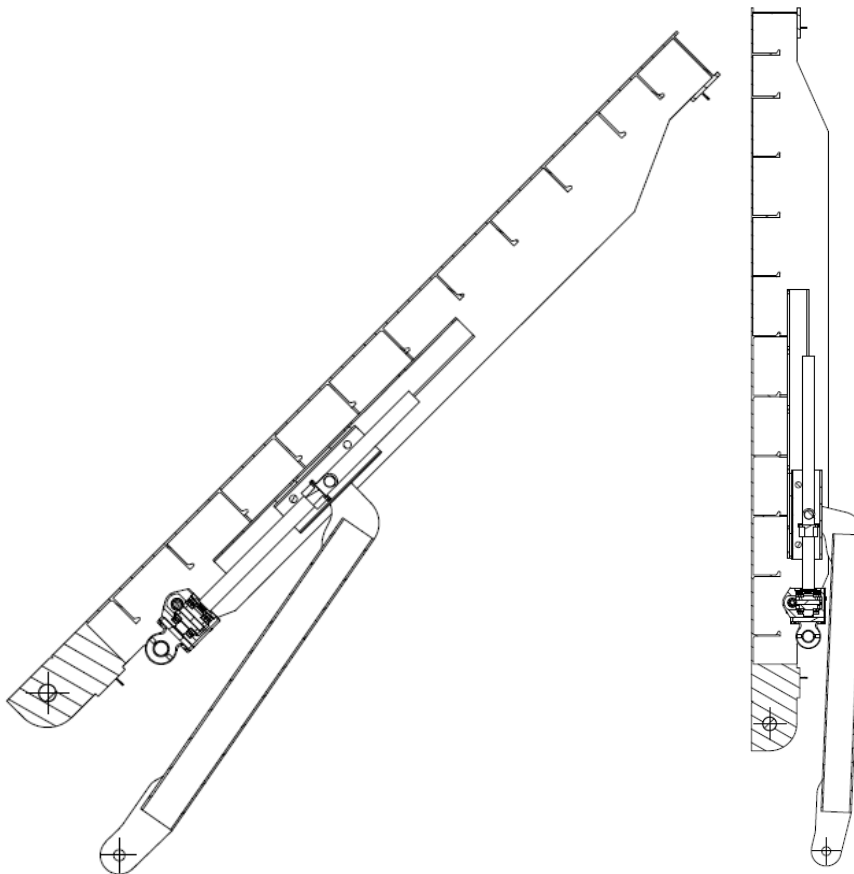


Figure 5.3: Ramp cover halfway open and completely open

The screw jack spindle does not need to withstand buckling during the opening operation but the forces required to lift the ramp cover are almost the same as when using the current hydraulic design due to the angle between the push rod and spindle being small.

The diagram in Figure 5.5 was drawn by using the calculations found in Appendix B with the inputs from Figure 5.4. The diagram describes how the force in the spindle F_{rod} changes with the cover's opening angle θ . As it can be seen F_{rod} is highest at the beginning of the opening operation, it decreases slowly until $\theta \approx 45^\circ$ and between $\theta \approx 45^\circ \rightarrow 90^\circ$ its rate of decrease accelerates.

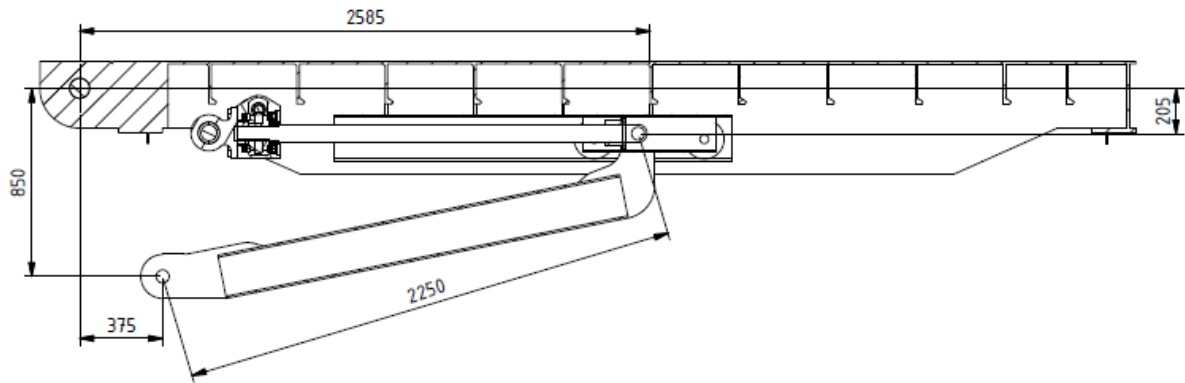


Figure 5.4: Dimensions of the final concept

The dimension 2585 mm corresponds to the distance between the ramp cover's hinge and the ramp cover's center of mass. The mass of the ramp cover is 20300 kg.

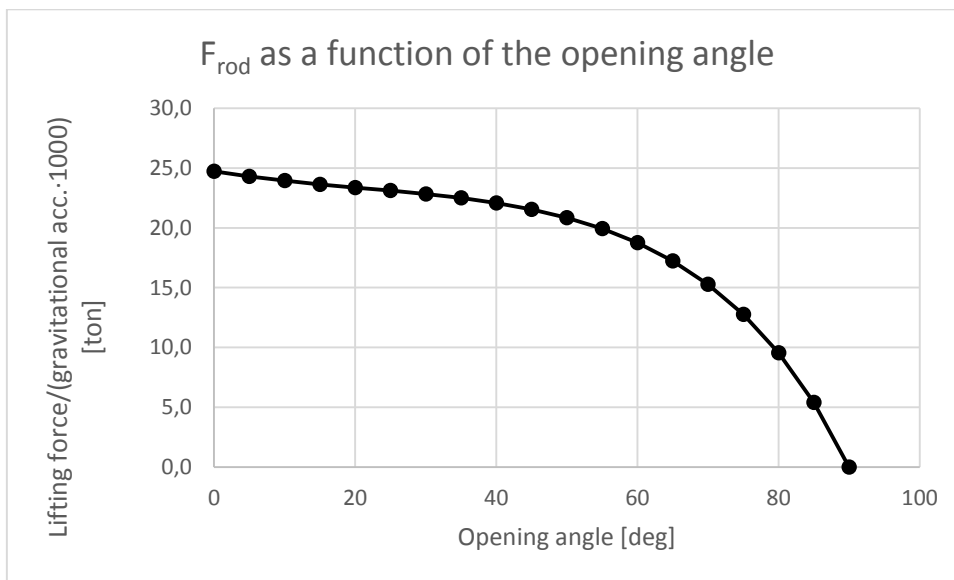


Figure 5.5: Diagram of F_{rod} as a function of the opening angle

To clearly illustrate all dimensions and components of the chosen concept they have been split into subsystems in the following text. These subsystems are described more thoroughly in Appendix B.

5.1.1 Screw jack

To pull the wagon along the track a screw jack will be used for example PMC Swedrive's. This screw jack can be seen in Figure 5.6. It will use a 18 kW motor (3 phase 400 V, 60 Hz) which will make the wagon move at a translational speed of about 710 mm/min. That gives an approximate opening time of the ramp cover of one and a half minute. This screw jack will pull the wagon with an initial (maximal) force corresponding to 25 ton, its stroke is 1,1 m (see Appendix B) and the spindle will be about 1400 mm long and has a diameter of 80 mm [4].

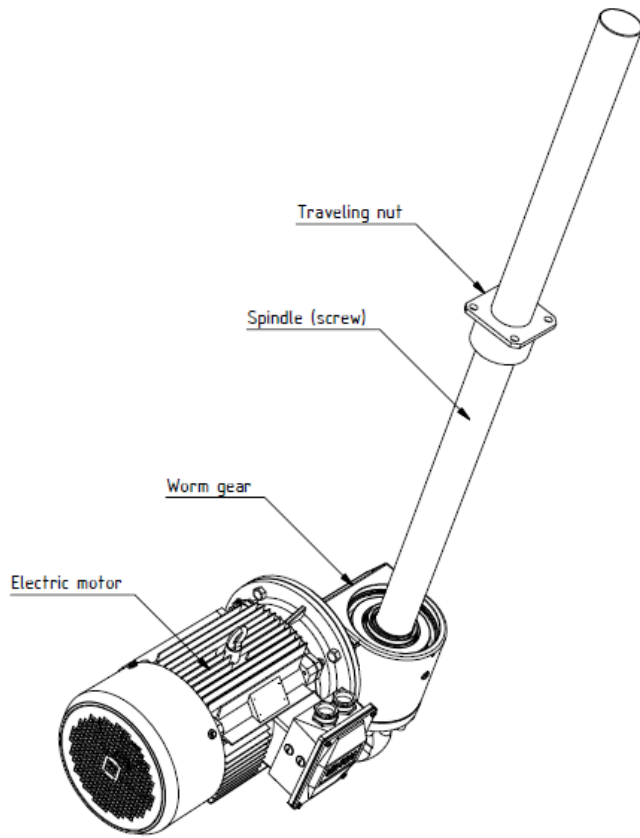


Figure 5.6: Isometric view of Screw jack and its traveling nut [4]

5.1.2 Wagon

Figure 5.7 shows a representation of the wagon that will slide in the guide track. This wagon is connected to both the screw jack (by way of the traveling nut) and the push rod. Pos. 1 shows the location of the traveling nut and pos. 2 shows the location of one of the guide pads. Guide pads are used instead of wheels because the loss due to friction corresponds to approximately 0,5 ton (see Appendix B), which is acceptable. The usage of guide pads is preferable since they are less expensive. Pos. 3 shows one of the holes for connection with the push rod.

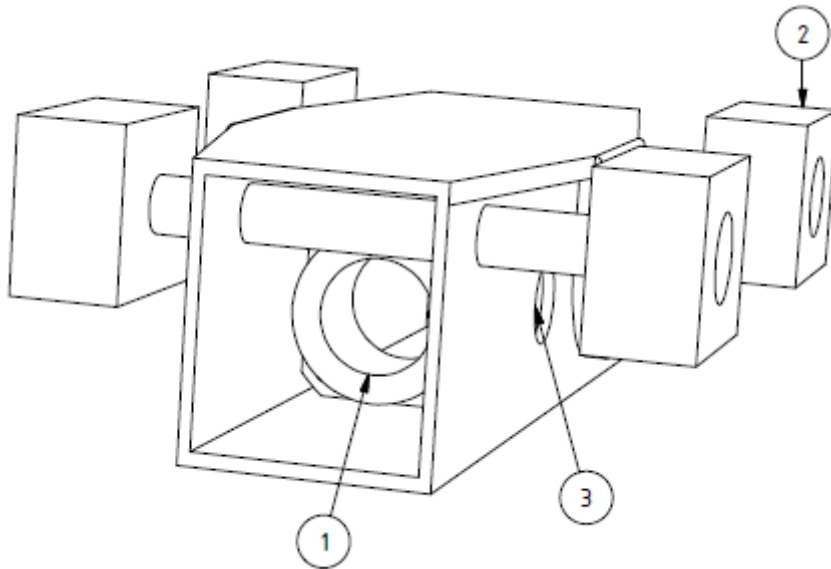


Figure 5.7: View of the wagon

5.1.3 Push rod

An isometric view of the rod can be seen in Figure 5.8.

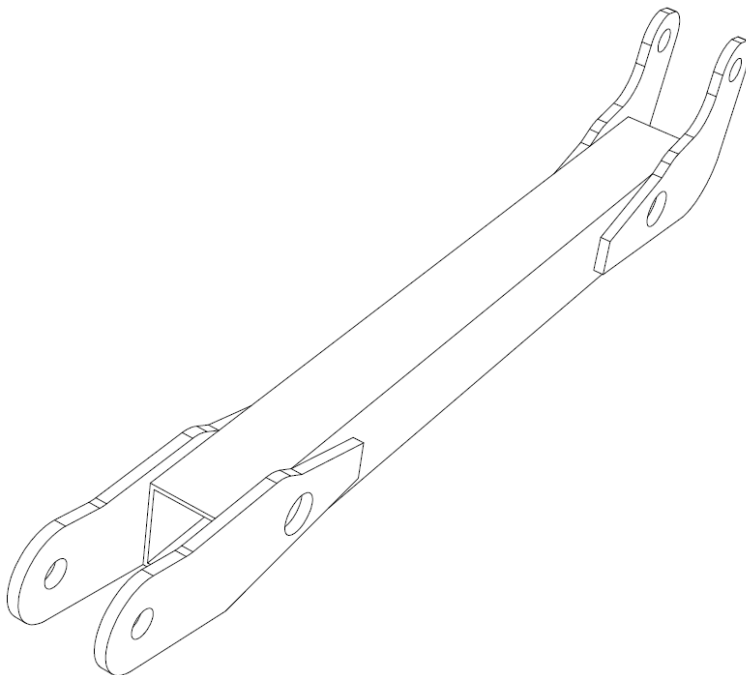


Figure 5.8: Isometric view of the rod

The push rod has a curved shape so it won't come in contact with the worm gear and the motor during the opening operation. It has also been dimensioned to: withstand plastic deformation, see Appendix B, not take too much space under the ramp cover and be wide enough to be fastened to the wagon.

5.1.4 Guide track

Figure 5.9 shows the guide track where the wagon will glide in. The holes at the top of the track are constructed to facilitate the installation, maintenance of the components that will be fitted in the track (seen in Figure 5.7) and the welding of the ribs (see Figure 5.10).

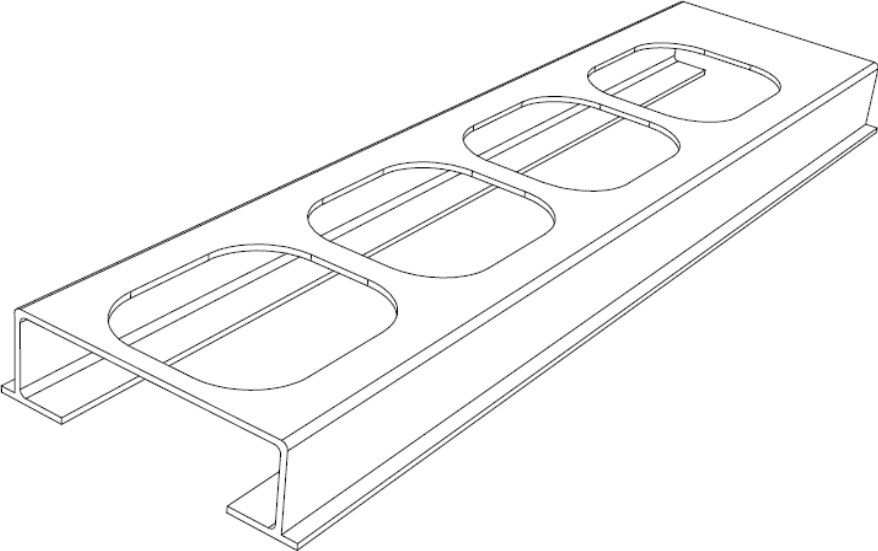


Figure 5.9: Guide track

Figure 5.10 below shows the ribs (pos. 1) that will be welded both to the track and to the longitudinal beams of the ramp cover. These ribs will add more structural stability to the track.

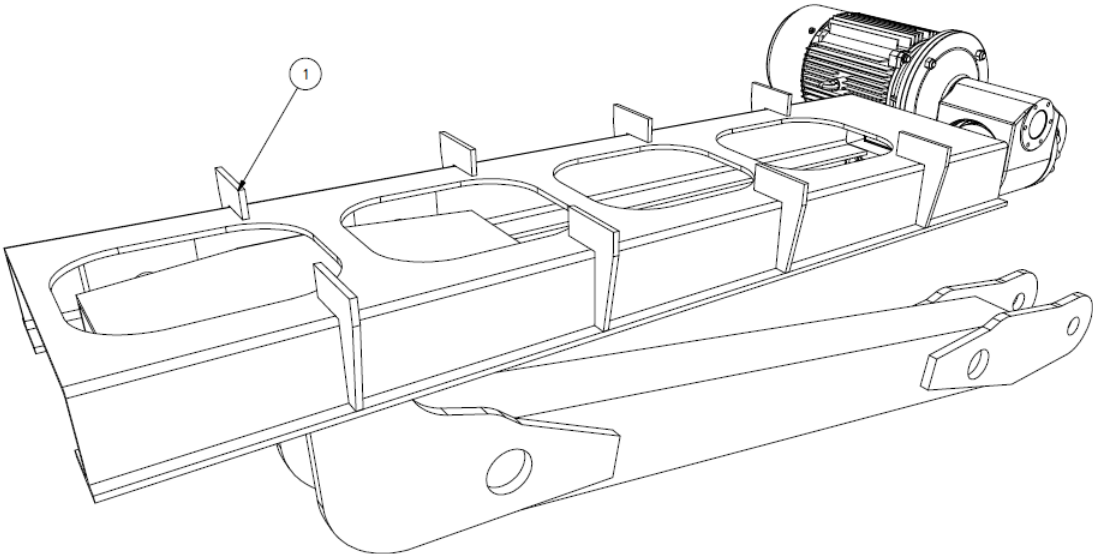


Figure 5.10: A view of the ribs to stabilize the track

Figure 5.11 shows the geometry of these ribs and how the guide track is formed. Pos. 1 shows a flange to where the rib will be welded to in order to prevent the guide track from deforming and “unfolding”.



Figure 5.11: Front view of the track and its supporting ribs

5.2 Cost review

The concept cost list can be found in Appendix D. There is also a more complete description of what components that have been taken into account and which haven't. All costs are approximate and have been estimated during discussions with relevant Design, Project & Purchase personnel inside TTS.

As seen in Appendix D, the new concept, Screw jack with push rod, and the current hydraulic design are equivalent to each other cost wise, about 265 000 SEK. In the same appendix can also be found costs for all the concepts that were analyzed.

6 Discussion

The final concept chosen is not a finished product, there are lots of work left before it can be released. All the dimensions seen in the figures are preliminary and the drawings in this report are not fully dimensioned, only the important dimensions have been drawn: the dimensions determined by the ramp cover's geometry; the dimensions critical in the equations related to the lifting force and the dimensions which ensure that all parts fit together.

The dimensions A and B, see Figure 4.1, should be maximized as much as possible. The dimension A is the one that has most influence in reducing the lifting force. A and B should be manipulated so that the lifting force per lift mechanism is kept under 25 ton. This because 25 ton lifting mechanisms seem to be the largest standard within the market.

In this report the ramp cover chosen was an average ramp cover, TTS has larger and smaller ones. For the larger ramp covers more than two lifting mechanisms could be used in order to stay under the 25 ton margin.

All equations used for all calculations can be found throughout the appendices. These equations are kept as general as possible in order to be able to change all the parameters, due to the wide range of ramp covers offered by TTS.

To reduce the lifting force as much as possible, the lifting mechanism should be placed on the opposite side of the ramp cover's hinge and the lifting force should be as perpendicular as possible to the ramp cover. This could be done for example by placing a winch mechanism on the deck above and hoist the ramp cover, see Figure E.2, but as mentioned in "7E.2 Winch ceiling" there are difficulties that need to be overcome in order for this system to work properly. This concept could be the topic of a future attempt to electrically maneuver a side hinged ramp cover.

7 Conclusions

To summarize, we think the *Screw jack with push rod* concept can be realized. The following conclusions can be presented:

- It will fulfil the technical requirements
- It will keep the same standard as the current hydraulic design
- Its cost is comparable to the hydraulic concept
- We recommend TTS to look into the chosen concept and develop it further

References

- [1] R. Valitsky: Leaking of the hydraulic, Maintenance Technology magazine, Henkel Corporation, 2014-01-13:
http://www.sbp.noaa.gov/resources/engineering/docs/Hydraulic_Systems_Leak_Free.pdf
- [2] Henrik Westermark (R & D Manager), TTS Marine AB
- [3] T. Dahlberg: Formelsamling i hållfasthetslära; Supplement till: Teknisk hållfasthetslära; 3rd edition, Studentlitteratur, Lund, 2001
- [4] Peter Rydh (Design Engineer), PMC Swedrive, 2014-04-02
- [5] Hamed Shakib (Structural Engineer), TTS Marine AB
- [6] Ramström transmission: Kedjekatalogen: Sektion: Lågfrikionsplast; Utgåva 4-2004
- [7] C. Ansel Ugural, K. Saul Fenster: Advanced mechanics of materials and applied elasticity; 5th edition, Prentice Hall, Westford, 2012
- [8] Tobias Ahlberg (Section Manager Design, Electrical/Hydraulics), TTS Marine AB
- [9] Henrik Adlersson (Project Estimator), TTS Marine AB
- [10] Joe Corbett (Piping Coordinator), TTS Marine AB
- [11] Peter Adolphsson (R & D Designer), TTS Marine AB

Appendix A. Existing Design

Figure A.1 below describes the geometry and the forces of the lifting mechanism of the existing side hinged ramp cover. Here q is the lever of the lifting rod and F_{lift} describes the lifting force from one hydraulic cylinder. The opening angle θ is the angle between the deck and the cover in an arbitrary position. The length x is the length between the hinge of the cover and its center of mass. A , B , c and b are constants and the symbols not mentioned are variables.

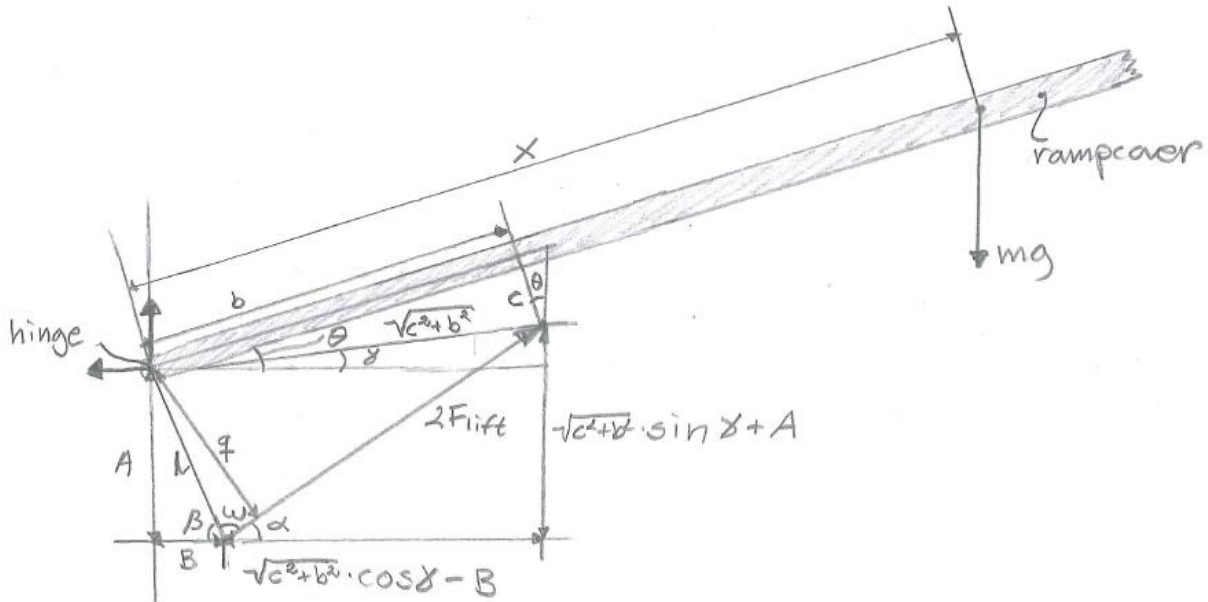


Figure A.1: Geometry of the ramp cover's transversal cross section, existing design (hydraulic)

A moment equilibrium around the ramp cover's hinge gives the following equation:

$$\sum M_{hinge} = 0 \Rightarrow 2F_{lift} \cdot q = mgx \cdot \cos(\theta) \Rightarrow$$

$$F_{lift} = \frac{mg \cdot x \cdot \cos(\theta)}{2 \cdot q} \quad \text{Equation A.1}$$

Equation A.1 is composed of the equations below which are formulated from the Figure A.1.

$$q = l \cdot \sin(\omega)$$

$$l = \sqrt{A^2 + B^2}$$

$$\omega = 180^\circ - \beta - \alpha$$

$$\beta = \arctan\left(\frac{A}{B}\right)$$

$$\alpha = \arctan\left(\frac{\sqrt{c^2 + b^2} \cdot \sin(\gamma) + A}{\sqrt{c^2 + b^2} \cdot \cos(\gamma) - B}\right)$$

$$\gamma = \theta - \arctan\left(\frac{c}{b}\right)$$

From the equations above a diagram was drawn, see Figure A.2. This diagram shows the lifting force F_{lift} (taken from Equation A.1), as function of the opening angle θ . The angles used were 0 to 90 degrees, where 0 represents the ramp cover in a closed position and 90 represents the ramp cover in an opened position.

The side hinged ramp cover used for the input parameters has article number A40705.

Inputs:

$$C = 0,33 \text{ m}$$

$$x = 2,3175 \text{ m}$$

$$A = 0,7 \text{ m}$$

$$B = 0,375 \text{ m}$$

$$b = 2,019 \text{ m}$$

$$\text{Mass of ramp cover } m = 20310 \text{ kg}$$

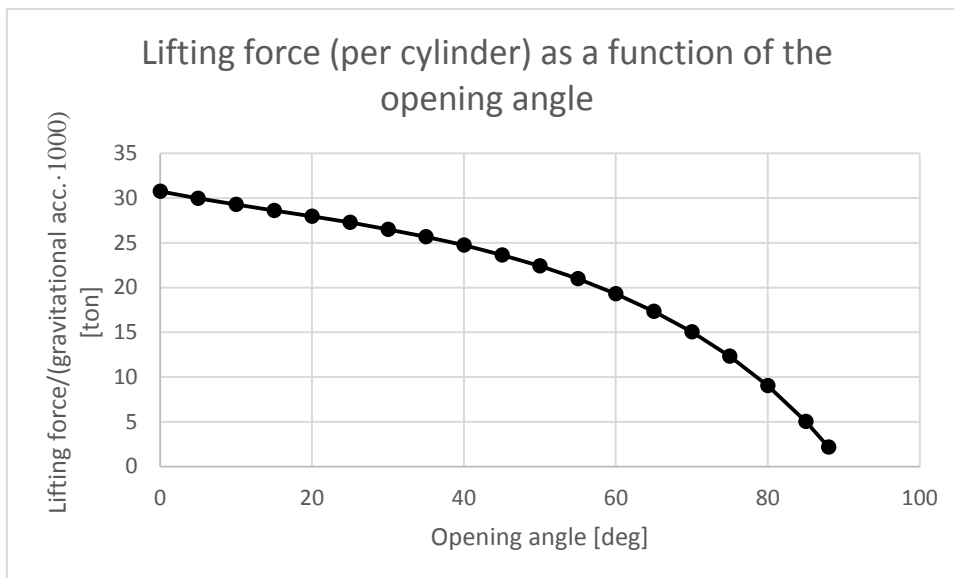


Figure A.2: Lifting force as a function of the opening angle

Appendix B. Screw jack with push rod – the final concept

From the brainstorming five concepts went through the first sorting process:

Infinity link, 3D rod, Winch with push rod, Direct pushing cylinder and Screw jack with push rod. Screw jack with push rod, chosen as the final concept, is analyzed more in "Screw jack with push rod". The headline below, *Sliding push rod*, is the lifting mechanism existing in four of the concepts mentioned above: *Infinity link, 3D rod, Winch with push rod* and *Screw jack with push rod*.

B.1 Sliding push rod

The concept *Sliding push rod* is used in all the concepts which went through the first sorting process: *Winch with push rod, Infinity link, 3D rod* and *Screw jack with push rod*. All of these solutions are driven by an electric motor. Three of the concepts can be combined with a screw jack or a mechanical cylinder, as seen in the box diagram below.

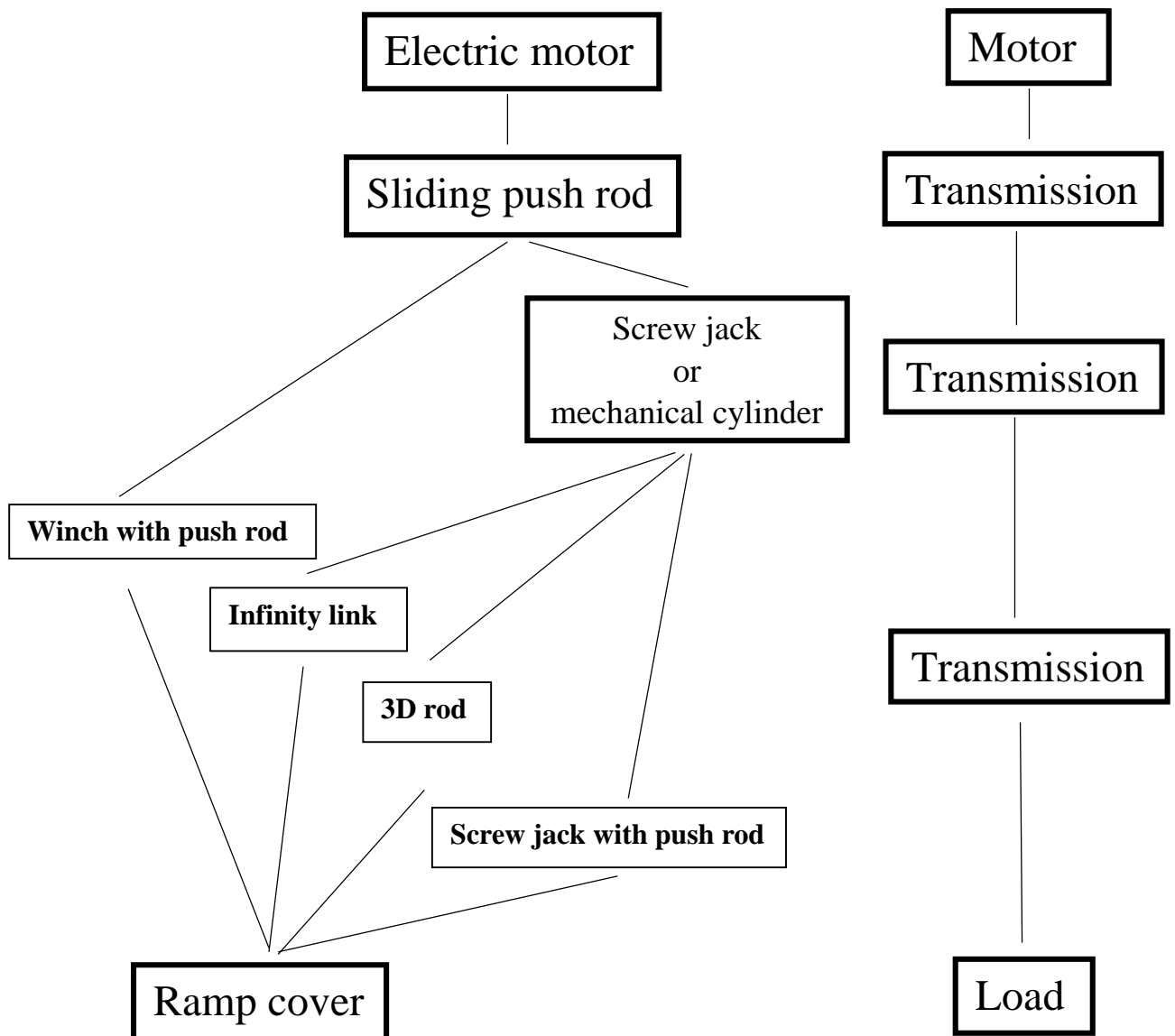


Figure B.1 below illustrates the geometry of the sliding push rod concept. The angle θ is the opening angle which is 0 when the ramp cover is closed and 90 when it's opened. L is the length of the lifting rod and the coordinate $S(\theta)$ describes the position of the point where the lifting rod is connected to the ramp cover in relation to the cover's hinge. This coordinate will vary as the angle θ varies. q is the lever used in the torque analyses for the lifting force F_{lift} and the lengths A and B describe the position of the hinge of the lifting rod in relation to the ramp cover's hinge.

Some values are always constant during the entire opening operation: A , B , L and c . These values are the inputs for the equation describing the opening process.

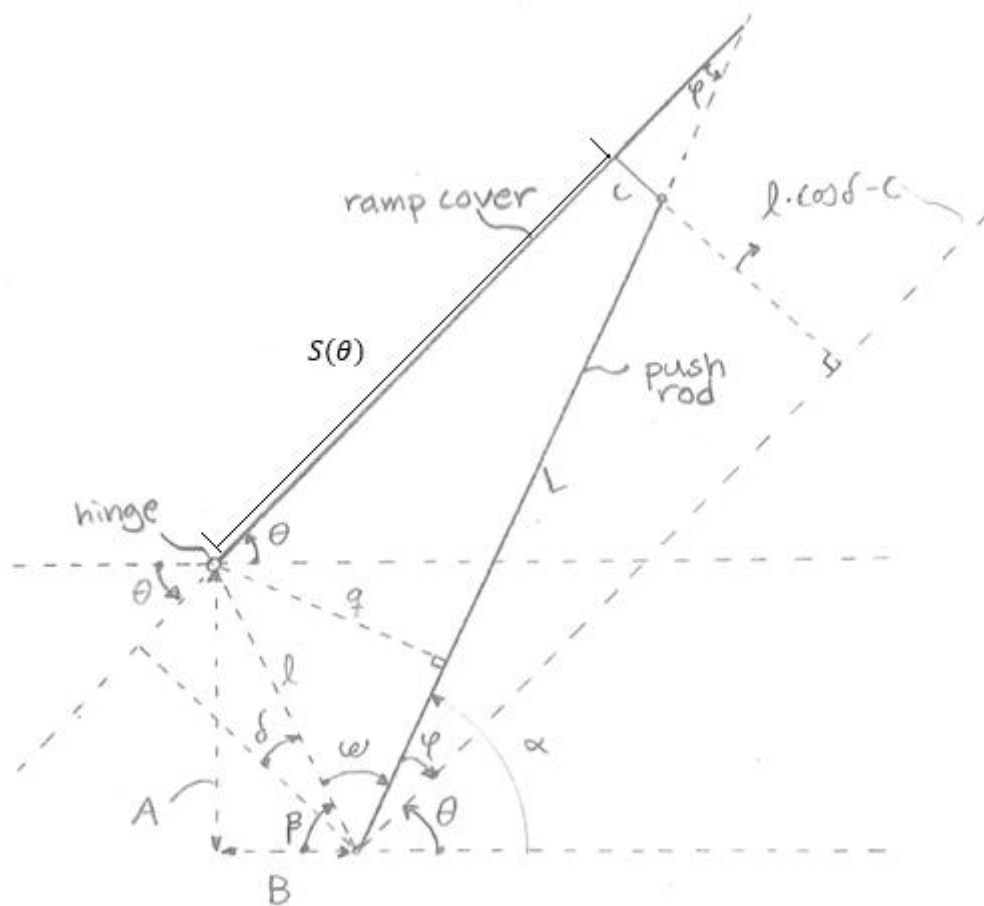


Figure B.1: Geometry of the ramp cover with constant length rod

The geometrical relations between the different forces can be seen represented in Figure B.2. F_{rod} is the force required to pull the rod towards the ramp cover's hinge and differs from F_{lift} by a factor $\cos(\varphi)$. These relations are described in Equation B.2 and Equation B.1.

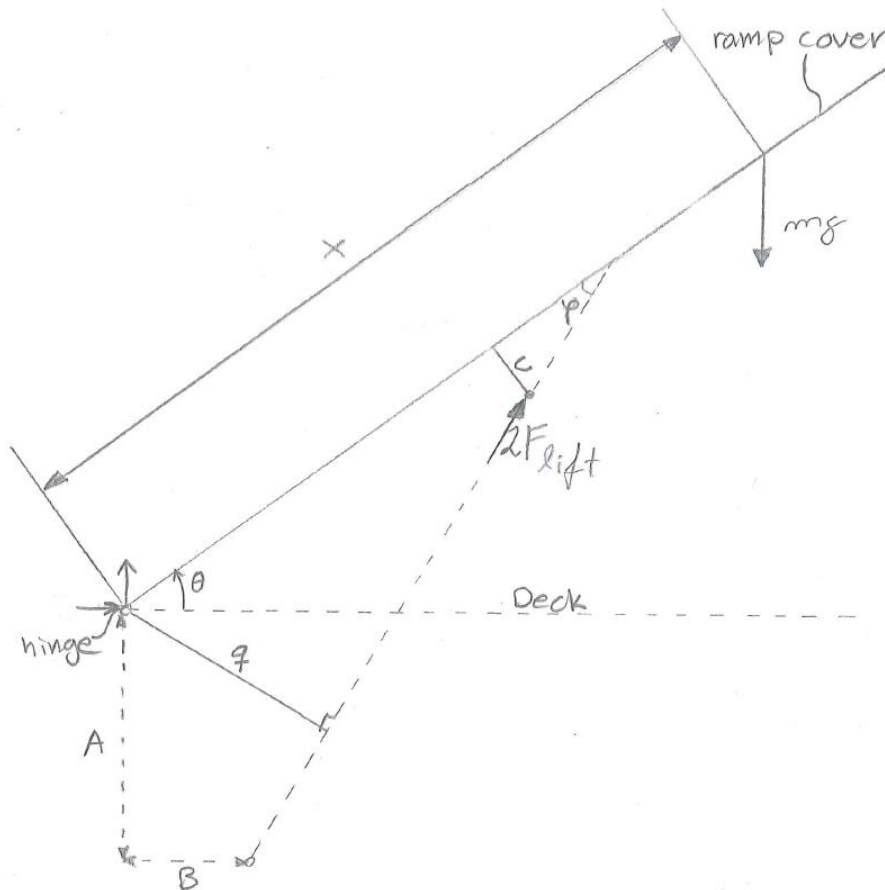


Figure B.2: Description of the forces involved under the opening operation

Equation B.1 has been constructed by analyzing the torque equation around the ramp-cover's hinge.

$$F_{lift}(\theta) = \frac{mg \cdot x \cdot \cos(\theta)}{2 \cdot q} \text{ Equation B.1}$$

Figure B.3 shows the translational mechanism positioned in point c, the mechanism ensures that the push rod will slide along the ramp cover. The figure illustrates the forces involved during the opening operation.

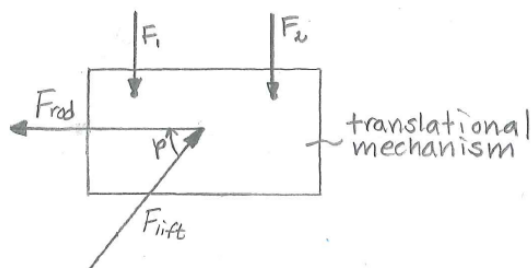


Figure B.3: Translational mechanism

A static force analysis in the direction of F_{rod} yields the following equation:

$$F_{rod}(\theta) = F_{lift}(\theta) \cdot \cos(\phi) \text{ Equation B.2}$$

B.1.1 Calculations to describe the lever q

The calculations down below describe how the lever q (in Figure B.1 above) vary with the opening angle θ .

$$q = l \sin(\omega)$$

$$l = \sqrt{A^2 + B^2}$$

$$\omega = 180^\circ - \beta - \alpha$$

$$\beta = \arctan\left(\frac{A}{B}\right)$$

$$\alpha = \varphi + \theta$$

$$\varphi = \arcsin\left(\frac{l \cos \delta - c}{L}\right)$$

$$\delta = 90^\circ - (90^\circ - \theta + (90^\circ - \beta)) \Leftrightarrow \delta = \theta - 90^\circ + \beta$$

The diagram shown in Figure B.4 describes how F_{rod} changes with the opening angle θ with the following inputs (side hinge ramp cover, article no. A40705):

$$x = 2,3175 \text{ m}$$

$$\text{Mass of ramp cover} = 20310 \text{ kg}$$

$$A = 0,85 \text{ m}$$

$$B = 0,375 \text{ m}$$

$$c = 0,26 \text{ m}$$

$$L = 3 \text{ m}$$

As it can be seen F_{rod} is highest at the beginning of the opening operation, it decreases slowly until $\theta \approx 45^\circ$ and between $\theta \approx 45^\circ \rightarrow 90^\circ$ its rate of decrease accelerates.

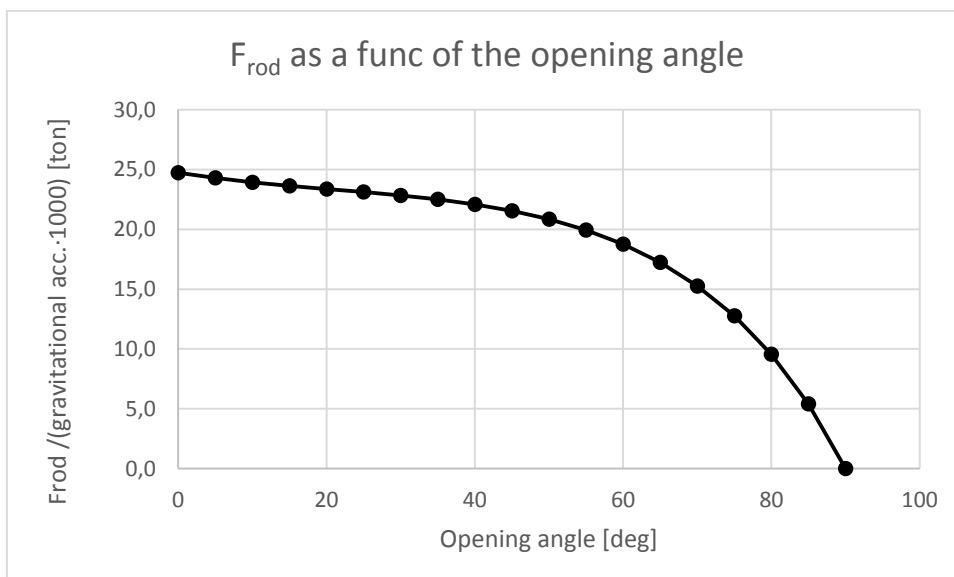


Figure B.4: F_{rod} as a function of the opening angle

Equation B.3 describes the stroke of the translational mechanism, the distance it has to move along the track.

$$S(\theta) = L\cos(\varphi) - l\sin(\delta) \text{ Equation B.3}$$

B.2 Screw jack with push rod

Of all the concepts analyzed further the screw jack with push rod was chosen as the final concept because of its simplicity and cost efficiency. This concept has been divided into the following subsystems: push rod, guide track, wagon, traveling nut and guide pads. These subsystems are described in the following text.

B.2.1 Push rod

The push rod has a curved shape, see Figure B.5, so it won't come in contact with the worm gear and the motor during the opening operation. It has also been dimensioned to withstand plastic deformation. The push rod must not take too much space under the ramp cover and be wide enough to be fastened to the wagon, which results in the inner width of 170 mm. Figure B.5 illustrates the most significant dimensions of the rod. The rod can be dimensioned in several different ways and Figure B.5 shows one possible solution. These dimensions ensures the rod complies with the requirements mentioned above.

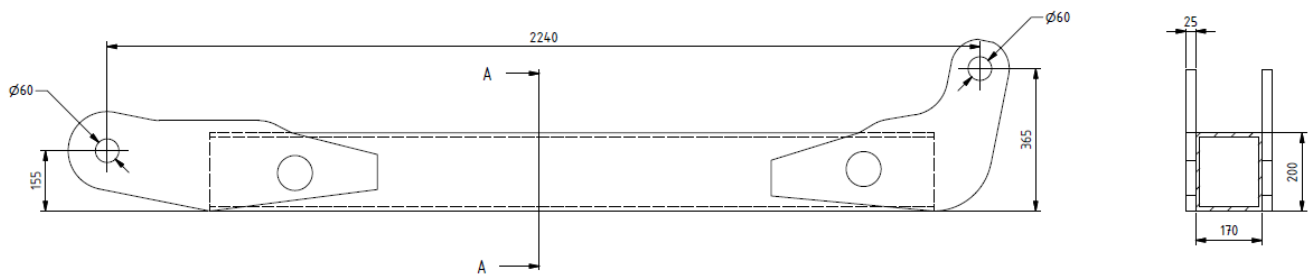


Figure B.5 Drawing of the rod

The rod will be manufactured by extruding a straight rectangular section and by welding the ears to straight section. Figure B.6 shows a hole made on an ear which will increase the amount of weldable surface between the ear and the straight section.

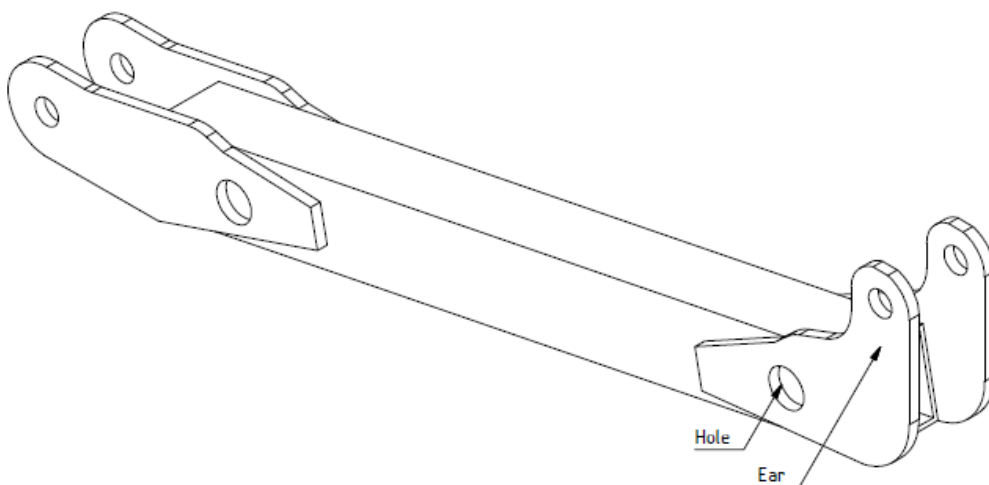


Figure B.6: Drawing of the rod

In order to examine how the rod would react to the stresses in the beginning of the opening operation (F_{rod} is maximal here) a model was made and examined in the stress analysis module of AutoDesk Inventor. Since buckling was a concern the most relevant place was the middle of the beam. As Figure B.7 shows, the Von Mises stress is very low in the middle of the beam (123,5 MPa) which is seen as acceptable [5]. As seen in the figure the stresses are high by sharp corner but can easily lowered by rounding the corners. The stress on the ears to the right are extremely high due to the constraint used on them. The constraint used is called frictionless and it was used to simulate the deformation of the rod correctly (Euler's case 2a, [3]).

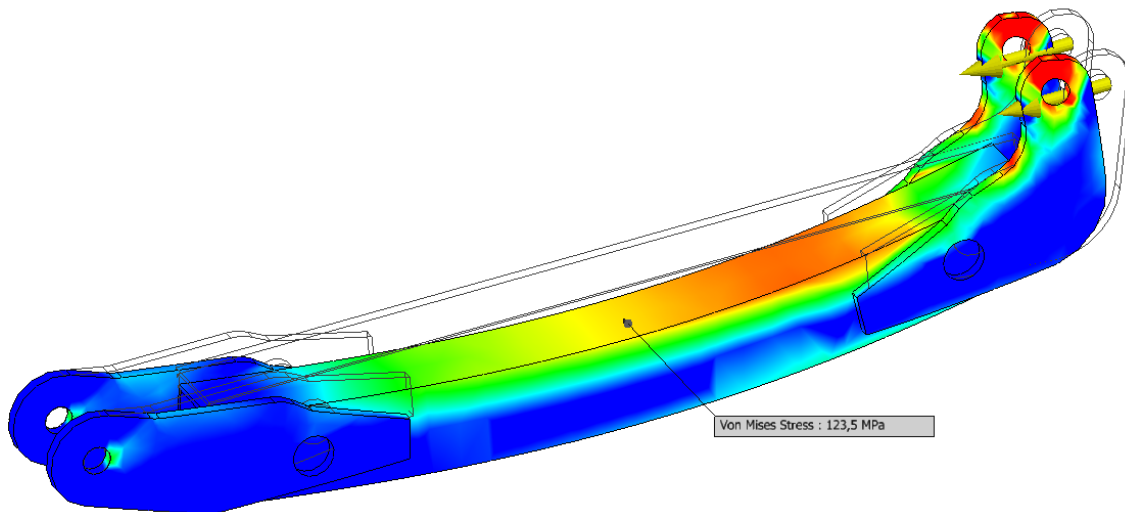


Figure B.7: Results from the stress analysis of the rod

B.2.2 Guide track

Figure B.8 shows some dimensions of the guide track in which the wagon will slide along. These dimensions were decided in order to get the wagon and its guide pads to fit in the guide track.

Because the stroke of the spindle is about 1,1 m, according to Equation B.3, the track needs to be about 1800 mm long in order for the wagon to stay within the guide track during the opening and closing operations.

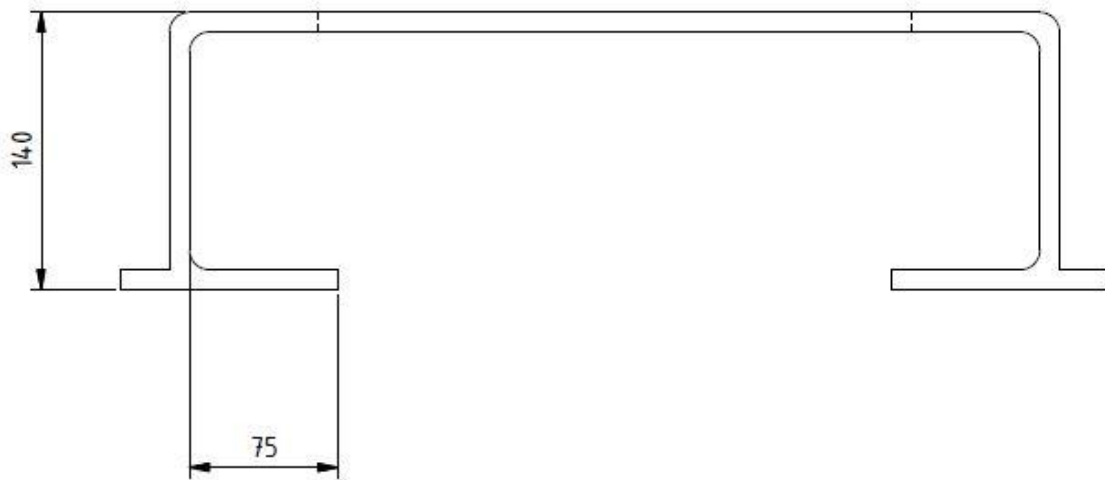


Figure B.8: Frontal view of the track

B.2.3 Wagon

Figure B.9 shows the wagon that will slide in the guide track. The wagon is connected to both the screw jack via the traveling nut and the push rod.

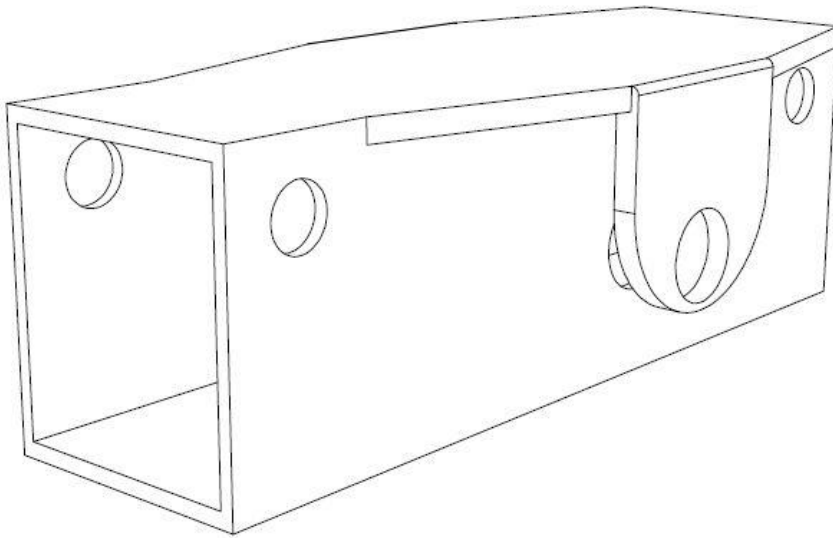


Figure B.9: Wagon

Figure B.10 is a representation of an arbitrary wagon. In order to analyze the forces acting upon it, Figure B.11 was made. Figure B.11 is an arbitrary representation of where the different axels will be positioned in the wagon and the forces which will act upon them. A, B, C and E describe the positioning of each axel in comparison to each other, the forces F_1 and F_2 are per axle. Pos. 1, 2, 3, 4 can be seen both in Figure B.10 and Figure B.11

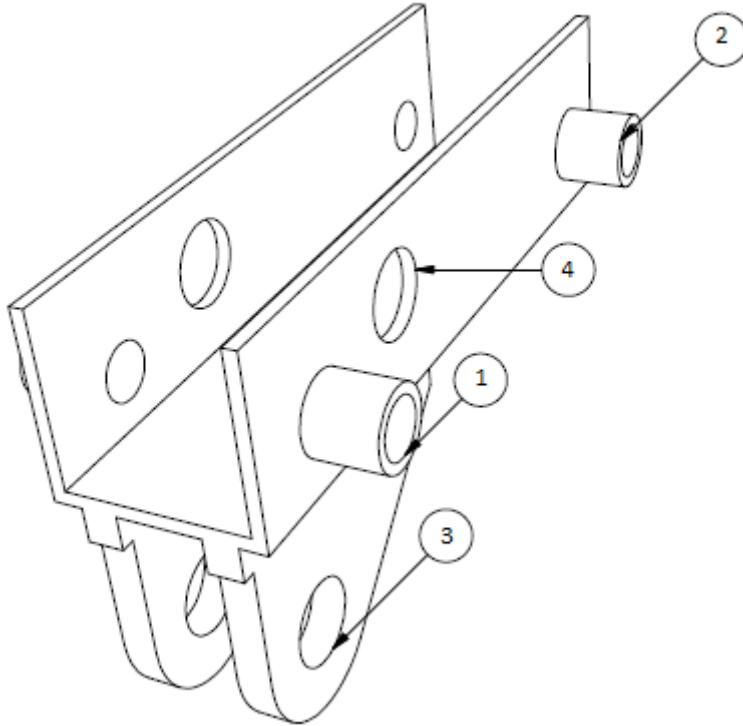


Figure B.10: Arbitrary representation of a wagon

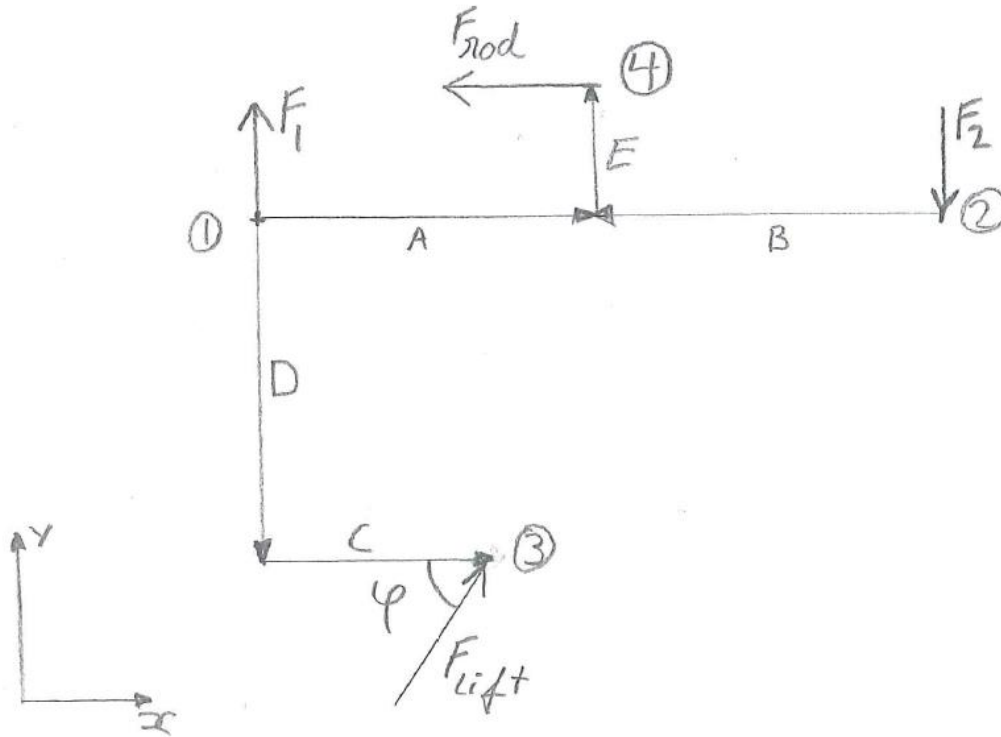


Figure B.11: Arbitrary positioning of the different axels in the wagon

A static force equation in the y- and x-direction yields the following equations:

$$F_1 - F_2 + F_{lift} \cdot \sin \varphi = 0 \text{ Equation B.4}$$

$$F_{lift} \cdot \cos \varphi = F_{rod} \text{ Equation B.5}$$

A moment equation around point 1 with Equation B.5 inserted gives:

$$-F_2 \cdot (A + B) + F_{lift} \cdot \cos \varphi \cdot E + F_{lift} \cdot \sin \varphi \cdot C + F_{lift} \cdot \cos \varphi \cdot D = 0 \Leftrightarrow \text{Equation B.6}$$

$$F_2 = \frac{F_{lift} \cdot \cos \varphi \cdot (E + D) + F_{lift} \cdot \sin \varphi \cdot C}{(A + B)} \text{ in Equation B.4 gives:}$$

$$F_1 = \frac{F_{lift} \cdot \cos \varphi \cdot (E + D) + F_{lift} \cdot \sin \varphi \cdot C}{(A + B)} - F_{lift} \cdot \sin \varphi \text{ Equation B.7}$$

Figure B.12 shows the dimensions pertaining to the positioning of the holes for the axels which were chosen by optimizing the parameters of Equation B.6 and Equation B.7 in order to achieve symmetrical wear on the guide pads. Some dimensions were chosen in order to make the wagon fit with the other parts, for example the wagon's width was adapted so the traveling nut sitting in the wagon will fit. The ears seen in Figure B.12 are there in order to reduce the deformation on the rest of the wagon.

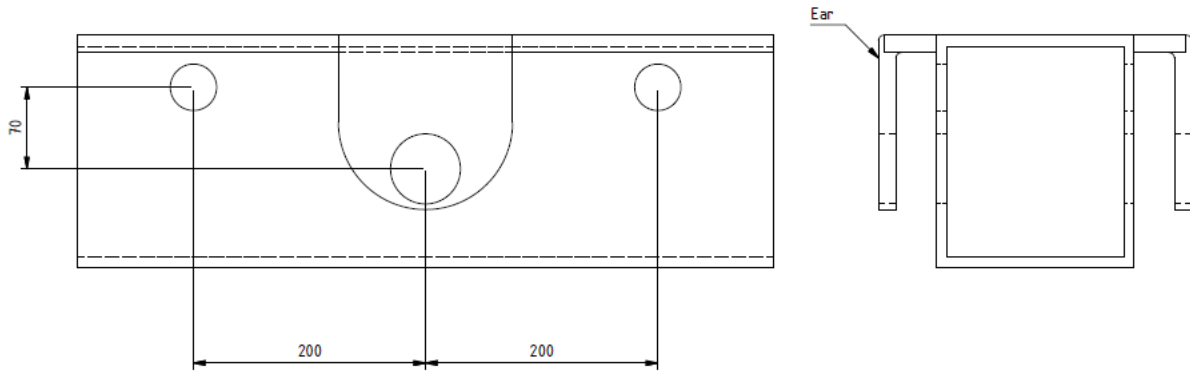


Figure B.12 Drawing of the wagon

With the dimensions according to Figure B.12:

- $A = 0,2$ m
- $B = 0,2$ m
- $C = 0,2$ m
- $E = -0,07$ m
- $D = 0,07$ m
- $F_{lift} = 25,6$ ton ($\theta = 0^\circ$)
- $\varphi = 15,2^\circ$

These values in Equation B.6 and Equation B.7 the forces F_1 and F_2 (see Figure B.11) become equivalent to -3,4 [ton] for axel 1 and 3,4 [ton] for axel 2, respectively and were chosen to cause a symmetrical wear on the guide pads.

To determinate if some kind of sliding system should be used, the following equation should be studied:

$$F_{friction} = \mu \cdot (F_1 + F_2) \text{ Equation B.8}$$

there $F_{friction}$ is the loss due to friction.

If $F_{friction}$ has a sufficiently low value guide pads can be used.

B.2.4 Traveling nut

Figure B.13 below shows the traveling nut which will make the wagon move along the spindle. It will pivot around an axle going through the wagon to minimize the spindle exposure to bending.

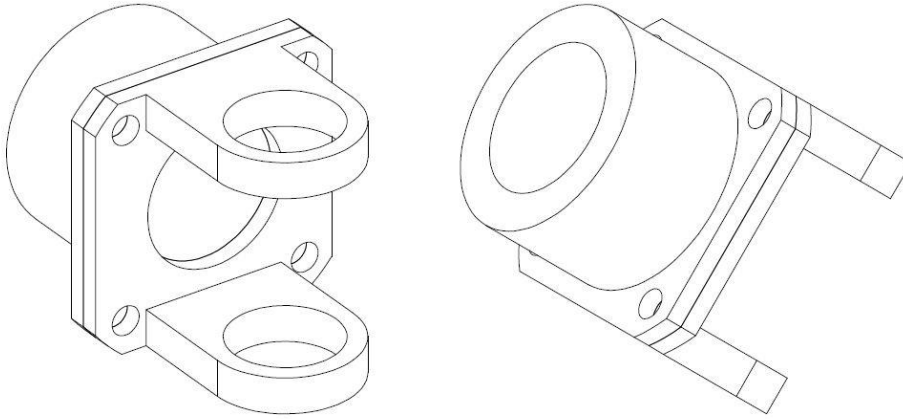


Figure B.13: Traveling nut

B.2.5 Guide pads

Figure B.14 shows two views of a guide pad. Guide pads will be used instead of wheels since the loss due to friction is rather low.

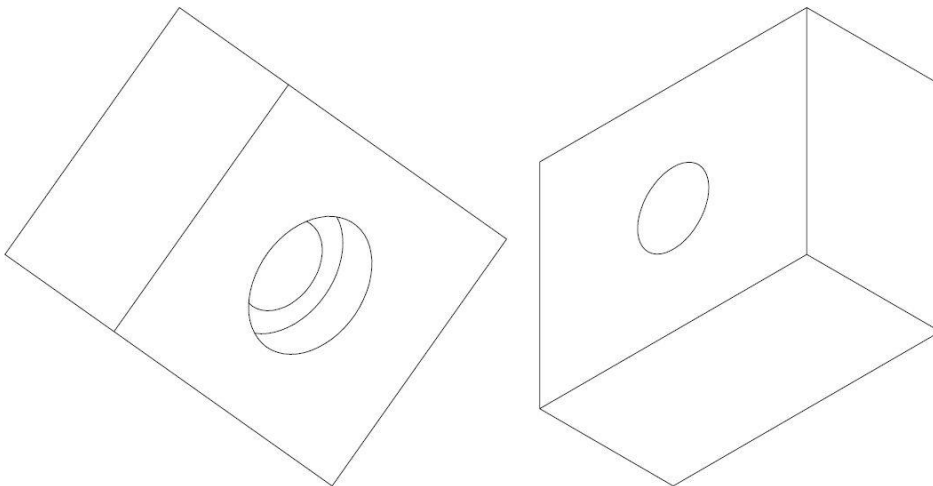


Figure B.14: Isometric views of one guide pad

Figure B.15 illustrates the dimensions of the guide pads relevant to avoid plastic deformation due to the stress between the guide pads and the guide track.

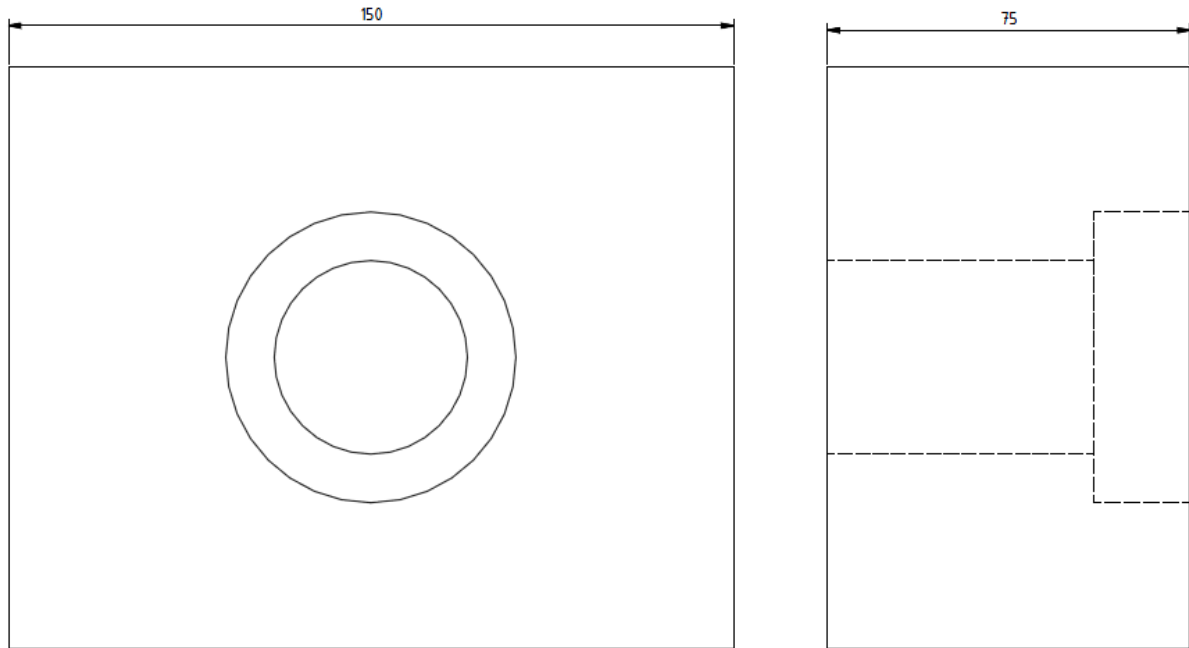


Figure B.15: Dimensions of the guide pads

The minimal area required for the guide pad is:

$$A_{min} = \frac{F_{1,2}}{\sigma_y} = \frac{16677}{22 \cdot 10^6} = 758 \text{ mm}^2$$
, where 22 [MPa] is the yield strength of the plastic PEHD 1000 REG [6], used here due to its low friction coefficient. $\frac{F_{1,2}}{2} = 16677$ [N] is the maximal load a single guide pad will be exposed to according to Equation B.6 and Equation B.7.

According to the dimensions in Figure B.15 the surface area of the guide pad is 11250 mm² which gives some safety margin against plasticity.

The friction between the guide pads and the steel track is 0,07 if lubricated PEHD 1000 REG is used [6]. With forces F_1 and F_2 , both corresponding to 3,4 ton, into Equation B.8 the loss due to friction becomes 0,476 [ton] during the first instance of the lifting operation.

The friction coefficient is dependent of so many variables so a conservative approach should be used here. The diagram in Figure B.16 illustrates how the loss due to friction would vary with different friction coefficients.

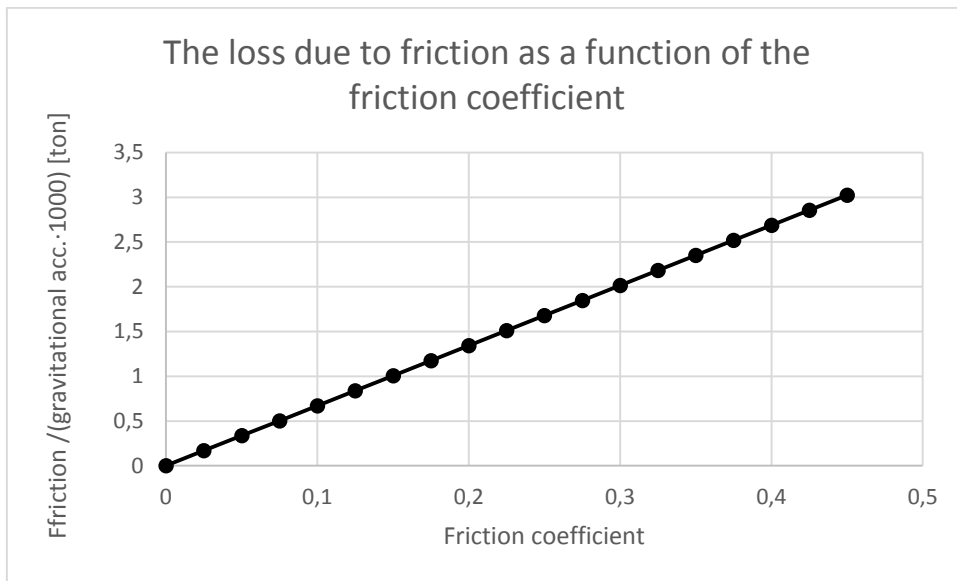


Figure B.16: Force diagram of the loss due to friction and the friction coefficient

Appendix C. Concepts analyzed further

C.1 Infinity link

This concept uses the sliding push rod platform where a linkage is used instead of a winch or a mechanical cylinder. The linkage is maneuvered by using a screw jack and its function is to force the linkage to either close or open (this screw jack including its driving motor cannot be seen in the figures below). This concept has the capability to reduce the initial lifting force but it loses its force reducing capability rather fast, see Figure C.3. Figure C.1 shows the concept when the ramp cover is closed and when it is 45 degrees open with its different components:

1. Ramp cover
2. Hinge
3. Lifting rod
4. Infinity link mechanism
5. Slider
6. Track

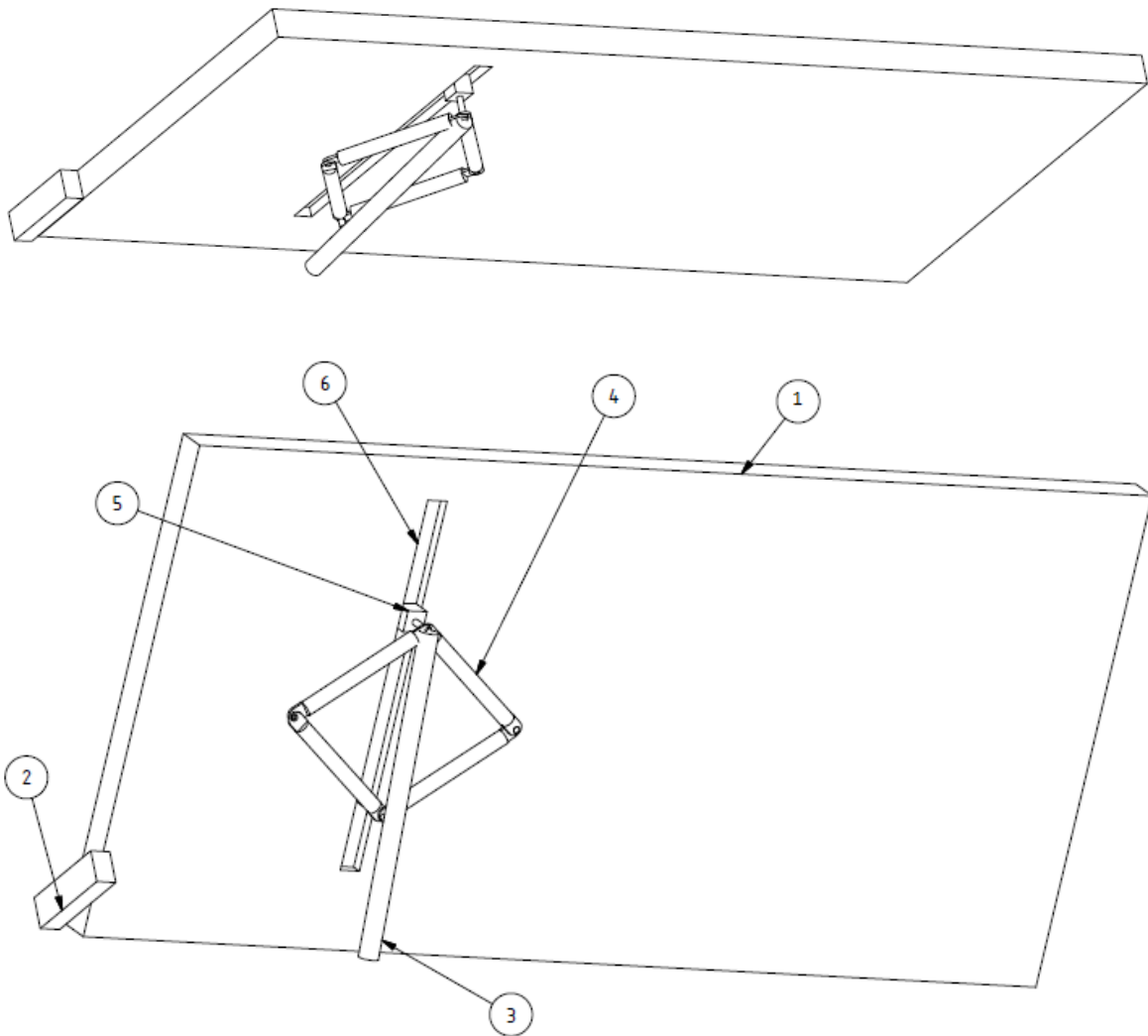


Figure C.1: Infinity link

$A = 0,7 \text{ m}$
 $B = 0,375 \text{ m}$
 $c = 0,33 \text{ m}$
 $L = 3 \text{ m}$
 Epsilon start = 85°
 $b = 1,2 \text{ m}$

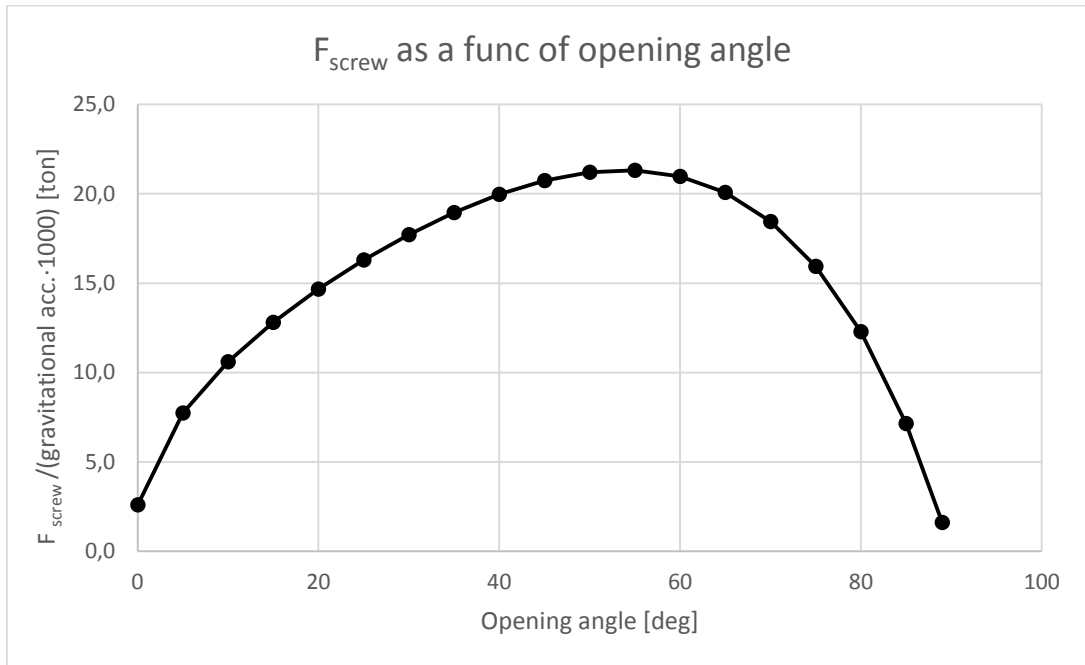


Figure C.3: F_{screw} as a function of the opening angle

S_{screw} describes the stroke of the screw.

$$S_{screw} = 2 \cdot (b \cos(\varepsilon(90)) - b \cos(\varepsilon(0))) \text{ Equation C.2}$$

C.1.1 Dimensioning of the cross section of the infinity link arm

In order to dimension the cross section of the arms of the infinity link a comparison between plasticity and buckling needs to be done in order to see which one of them is critical for deciding the dimensions.

To dimension the infinity link's arms against plasticity the following equation was used [7]:

$$\sigma_{yield} = \frac{P_{max}}{A_{min}} = \frac{P_{max}}{\pi r_{min}^2} \Leftrightarrow r_{min} = \sqrt{\frac{P_{max}}{\pi \cdot \sigma_{yield}}} \text{ where } P_{max} = \frac{F_{rod,max}}{2 \cdot \sin \varepsilon}$$

here $F_{rod,max}$ is the maximal force the link arm will encounter during the opening operation. ε is the corresponding angle in the linkage, see Figure C.2 and σ_{yield} is the yield strength of the chosen material.

To dimension the infinity link's arms against buckling the following reasoning was used:

The infinity link mechanism will be exposed to buckling when the closing operation is initiated (launching of the ramp cover). This will be exacerbated if the ship is leaning in an unfavorable way, as much as 5 degrees, see Figure C.5.

The force P_{Launch} is the force one arm will have to push the ramp cover with during the launching operation and P_{Launch} is described by Figure C.4 and the equations below:

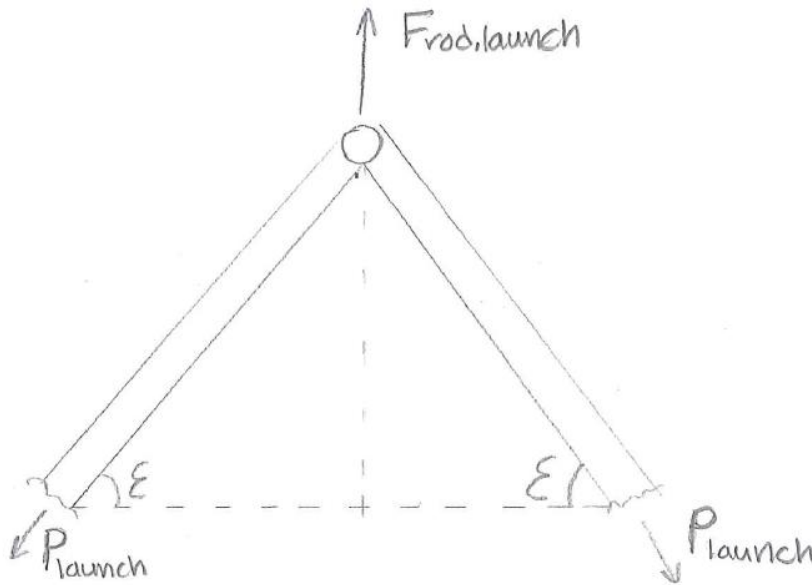


Figure C.4: Sketch representing the force situation during the launch of the ramp cover

$$P_{Launch} \cdot \sin \epsilon(90) + P_{Launch} \cdot \sin \epsilon(90) = F_{rod,launch} \Leftrightarrow P_{Launch} = \frac{F_{rod,launch}}{2 \cdot \sin \epsilon(90)}$$

there $F_{rod,launch} \approx \frac{mg \cdot x \cdot \sin 5^\circ}{2 \cdot q(90)}$ (see Figure C.5, Equation C.3 and Equation C.4 below)

where q is taken from “B.1.1 Calculations to describe the lever q ” with $\theta = 90^\circ$.
 x is the coordinate that describes the position of the center of mass of the ramp cover and
 m is the mass of the ramp cover.

Figure C.5 shows the geometry necessary to calculate P_{Launch} .

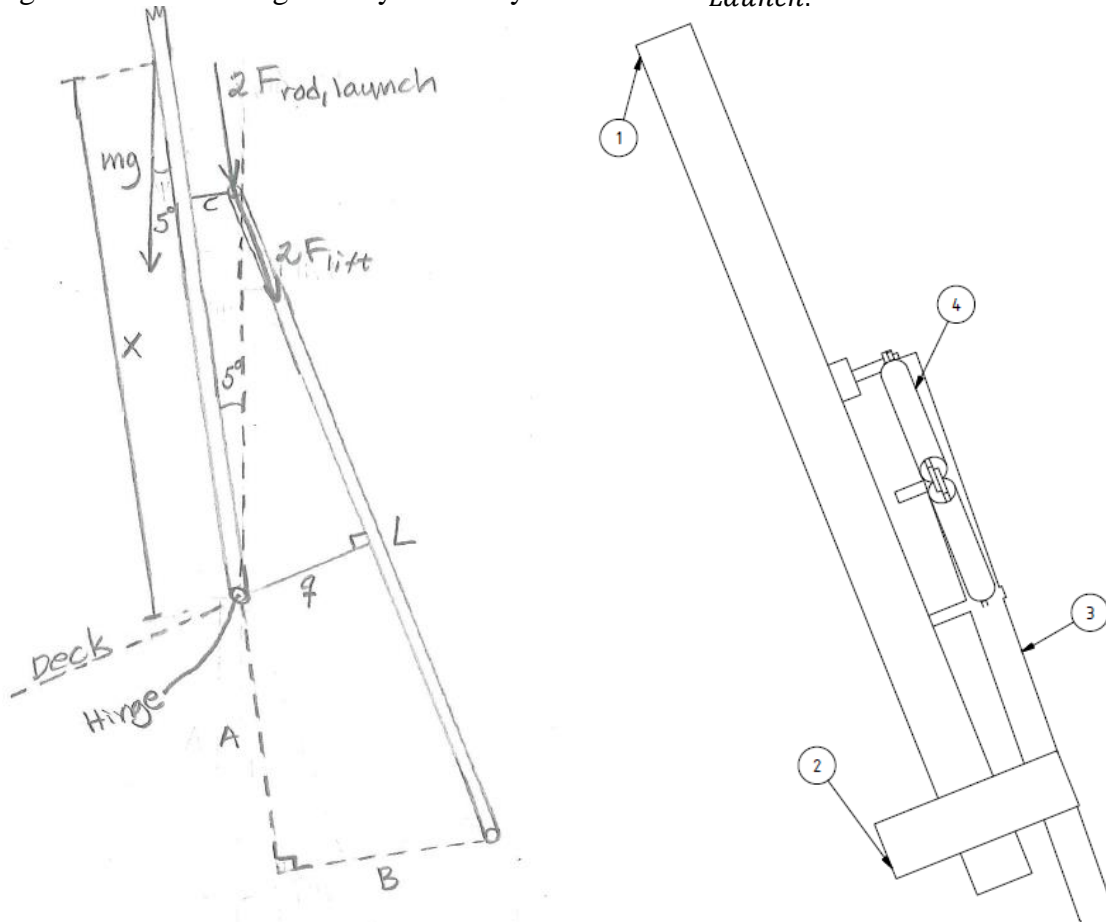


Figure C.5: Cross section of a ramp cover when the entire boat is leaning 5°

The figure above shows the different components for this concept:

1. Ramp cover
2. Hinge
3. Lifting rod
4. Infinity link

A moment equation around the ramp cover's hinge yielded:

$$2F_{lift} \cdot q(\theta) - mg \cdot x \cdot \sin 5^\circ = 0 \text{ Equation C.3}$$

$$F_{lift} = F_{rod, launch} \cdot \cos \varphi \text{ but since } \varphi \text{ is very small } \Rightarrow$$

$$F_{lift} \approx F_{rod, launch} \text{ Equation C.4}$$

Euler's buckling case nr. 2a [7] gives the maximal force a beam can be exposed to as:

$$P_{buckling} = \frac{\pi^2 \cdot E \cdot I}{L^2}$$

A comparison between this value and P_{Launch} should be made to ensure the arms will sustain the loads applied during the first instants of the closing operation.

C.1.2 Alternative infinity link

The infinity link solution is based on symmetry, all of the mechanism's arms have the same length. In this alternative solution the lengths a and b are different, see Figure C.6 below. This alternative solution was tested to see if any dimensions lowered the maximum opening force or if the opening force curve could be made smoother. In order to compare this alternative solution with the infinity link, the total length of the arms was restricted to be the same as the infinity link. These tests resulted in neither lower opening force nor the force curve to become flatter. It appeared that the best lengths of the arms were when they were all the same, as in the ordinary infinity link solution described earlier.

The alternative solution of the infinity link had exactly the opposite effect intended, it reduced the initial force even more than the normal infinity link and it became weaker even faster than the normal infinity link.

The inputs used were (compare with Figure C.6):

a = length of link arm

b = length of link arm

γ = angle between the link arms a and the horizontal plane

ε = angle between the link arms b and the horizontal plane

F_{screw} = screw force

F_{rod} = rod force

$S(\theta)$ = Stroke

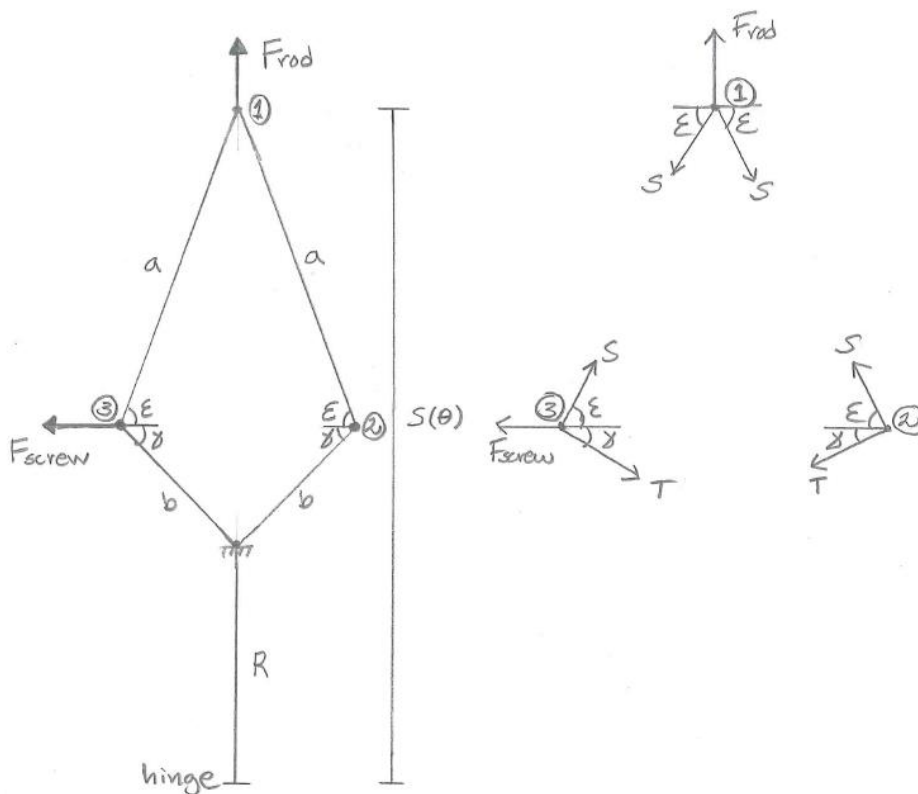


Figure C.6: Dimensions of the alternative infinity link and forces on joints 1, 2 and 3

From Figure C.6 the Equation C.5 and Equation C.6 can be set up:

$$a \cdot \sin(\varepsilon) + b \cdot \sin(\gamma) + R = S(\theta) \text{ Equation C.5}$$

$$\gamma = \cos\left(\frac{a \cdot \cos(\varepsilon)}{b}\right) \text{ Equation C.6}$$

Equation C.6 was inserted in Equation C.5 and ε was solved numerically with MatLab, the code can be found below.

To get F_{screw} as a function of F_{rod} the joints 1, 2 and 3 were exposed with all the acting forces and the following relations were established, see Figure C.6:

Joint 1 led to:

$$F_{\text{rod}} = 2 \cdot s \cdot \sin(\varepsilon) \text{ Equation C.7}$$

Joint 2 led to:

$$s \cdot \sin(\varepsilon) = T \cdot \sin(\gamma) \Rightarrow S = \frac{T \cdot \sin(\gamma)}{\sin(\varepsilon)} \text{ Equation C.8}$$

Joint 3 led to:

$$F_{\text{screw}} = s \cdot \cos(\varepsilon) + T \cdot \cos(\gamma) \text{ Equation C.9}$$

Equation C.8 in Equation C.7 resulted in:

$F_{\text{rod}} = 2 \cdot T \cdot \sin(\gamma)$, inserted in Equation C.9 resulted in the screw force:

$$F_{\text{screw}} = \frac{F_{\text{rod}}}{2} \left(\frac{\cos(\varepsilon)}{\sin(\varepsilon)} + \frac{\cos(\gamma)}{\sin(\gamma)} \right) \text{ Equation C.10}$$

The MatLab code below was used to calculate Equation C.5 and Equation C.10 numerically. For all input, see Figure C.6 ($\varepsilon_0 \equiv \varepsilon(0)$, $\gamma_0 \equiv \gamma(0)$ and $S_0 \equiv S(0)$ were used to get R).

```
clear all, clc

epsilon0=85*pi/180;      %initial angle
a=1;
b=1;
S0=3.35;                %S(0) stroke when theta is zero

gamma0=acos(a*cos(epsilon0)/b);
R=S0-(a*sin(epsilon0)+b*sin(gamma0));

S=[3.35 ; 3.29 ;3.22 ;3.15 ;3.08 ;3.01 ;2.94 ;2.87 ;2.80 ;2.74 ;2.68 ;2.62 ;2.56
;2.51 ;2.46 ;2.41 ;2.37 ;2.33 ;2.31 ;2.30]; %S is the stroke at different theta
angles

Frod=[63;60.7;58.7;56.8;55.1;53.3;51.6;49.8;47.9;45.8;43.4;40.7;37.6;33.9;29.5
;24.3;17.9;10;2.2;0]; %Frod at the points that coincide with S defined above

x0=1.5; %a guess required to use fzero
for i=1:20
```

```
f=@(x)a*sin(x)+b*sin(acos(a*cos(x)/b))+R-S(i);  
epsilon(i)=fzero(f,x0);  
gamma(i)=acos(a*cos(epsilon(i))/b);  
FscREW(i)=Frod(i)/2*((cos(epsilon(i))/(sin(epsilon(i)))+(cos(gamma(i))/(sin(gamma(i)))))); %The desired force  
x0=epsilon(i); %the new guess becomes the previous result  
end
```

C.2 3D rod

This concept utilizes the push rod, but instead of having a track that runs transversally the track's position and geometry will vary. The position of the track will define how the lifting force will vary during the lifting operation. Figure C.7 down below shows one example of how to place the track and how the lifting rod will behave during the opening operation.

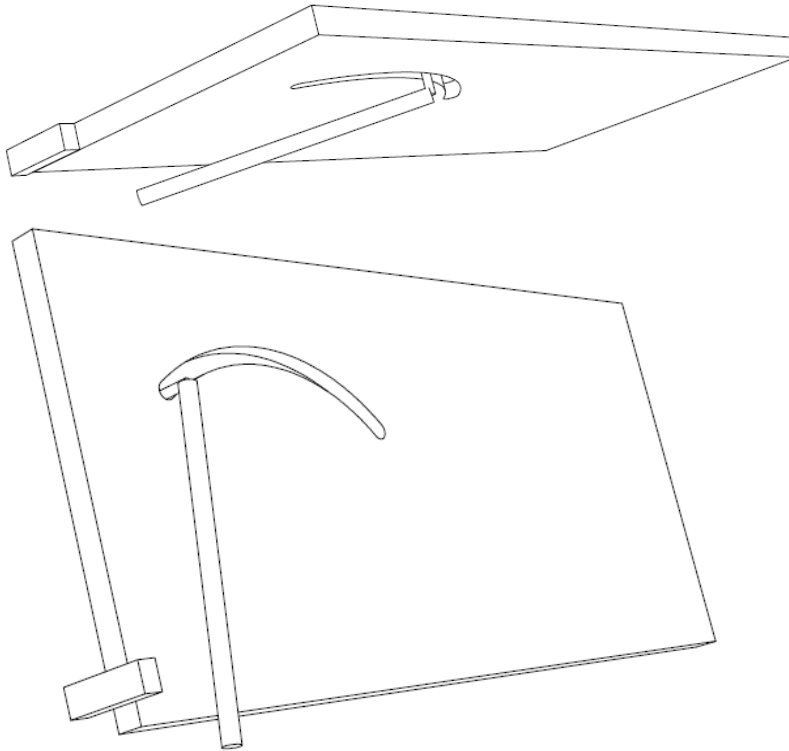


Figure C.7: 3D rod, opened and closed positions

It is difficult to find an optimal track, where the force required to lift the ramp cover is very low at the beginning. The concept is very weak at the beginning of the lifting operation and quite strong at the end as it can be seen in the diagram in Figure C.11 down below. This force situation is exactly the opposite of what is required.

The design, with different kind of geometries of the tracks, was hard to describe mathematically and this is the reason why one model was made in AutoDesk Inventor and analyzed in Dynamic Simulation.

The motion was created by adding a part that moved like a hydraulic cylinder (see Figure C.8 item number 6) and this part was constrained so it would perform its stroke under a full minute. The reason for adding this extra part to the simulation is due to the inability of Inventor's dynamic simulation to force a motion on a sliding cylinder curve joint. The hydraulic cylinder was created by making two cylinders: a hollow one and a massive one and were constrained by using a cylindrical joint.

Figure C.8 shows where the different components were positioned before analyzing the assembly in Dynamic Simulation:

1. Ramp cover
2. Hinge
3. Lifting rod
4. Slider
5. Guide track
6. "Hydraulic cylinder"

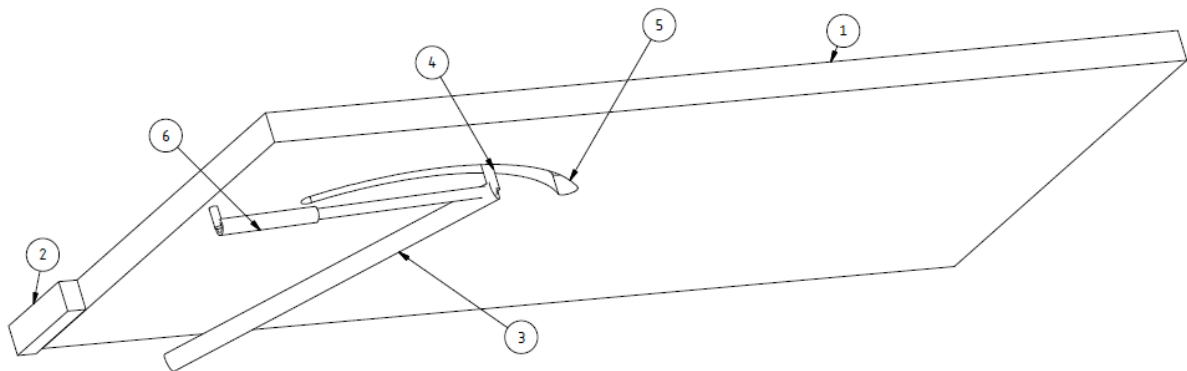


Figure C.8: Isometric view of the assembly used to simulate the 3D rod

Figure C.9 and Figure C.10 below show the geometry of the guide track, the point where the rod was placed (the point to the left in Figure C.9) and the point where the driving mechanism was placed (the point to the right in Figure C.9).

These points and the track were chosen arbitrarily since there is a large amount of different configurations possible.

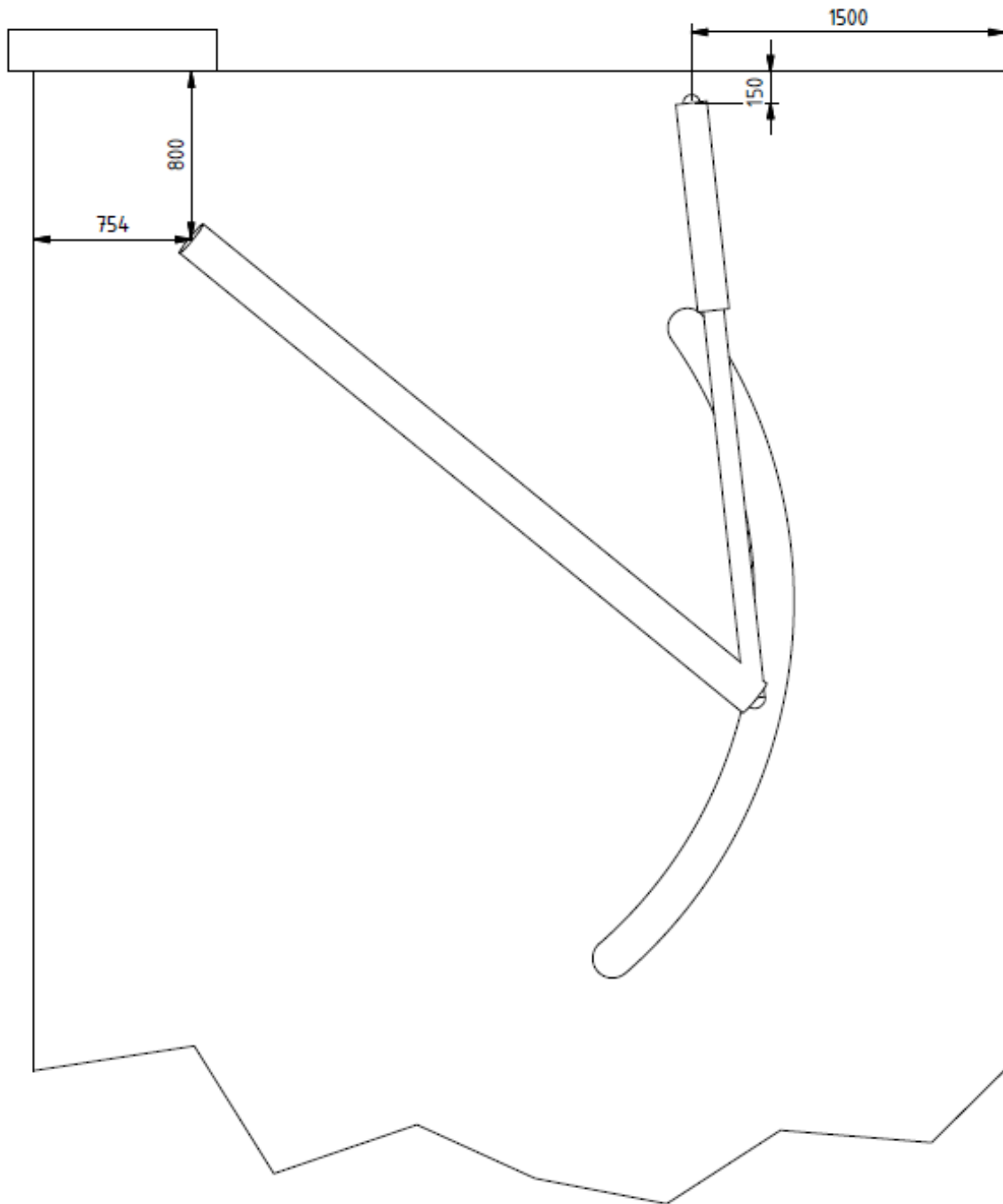


Figure C.9: Placement of the driving mechanism and lifting rod

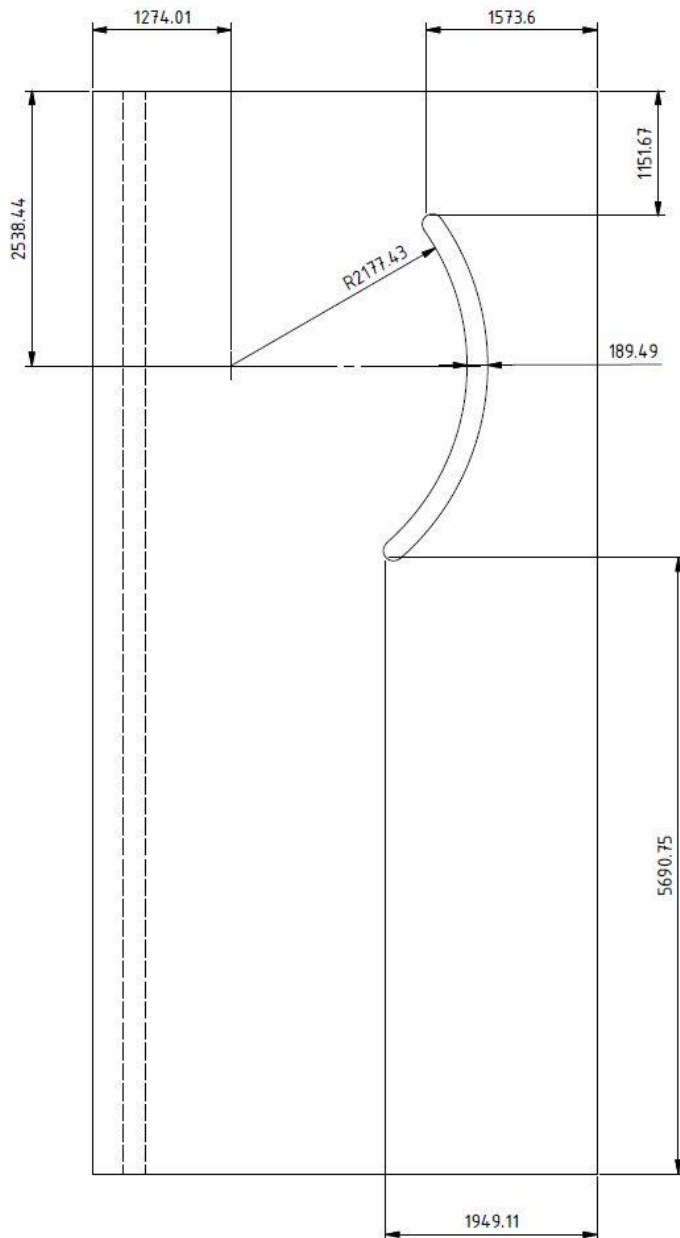


Figure C.10: Description of the geometry of the track

The following joints were used in Dynamic Simulation:

- Cylindrical between the ramp cover and the hinge.
- Spherical between the rod and its attachment against the ship's hull.
- Spherical between the rod and the slider.
- Sliding cylinder curve between the slider and the guide track (curve).
- Spherical between slider and the "hydraulic cylinder".
- Spherical between the "hydraulic cylinder" and the ramp cover.

This simulation was used to show how the lifting force varies during the lifting operation, only half a ramp cover was modelled to reduce the amount of complexity in the model.

The inputs (for side hinge ramp cover, article no. A405705) down below were used to get the diagram in Figure C.11:

$$x = 2,3175 \text{ m}$$

$$\text{Mass of ramp cover } m = 12500 \text{ kg}$$

$$A = 0,7 \text{ m}$$

$$B = 0,375 \text{ m}$$

$$c = 0,33 \text{ m}$$

$$L = 3 \text{ m}$$

The diagram in Figure C.11 illustrates how the lifting force changes as a function of time, as it can be seen, the mechanism is inefficient at the beginning of the opening operation since it requires a lot of force to lift the ramp cover. The diagram was obtained through using AutoDesk Inventor's Dynamic Simulation and it was plotted by using AutoDesk Inventor's Output Grapher.

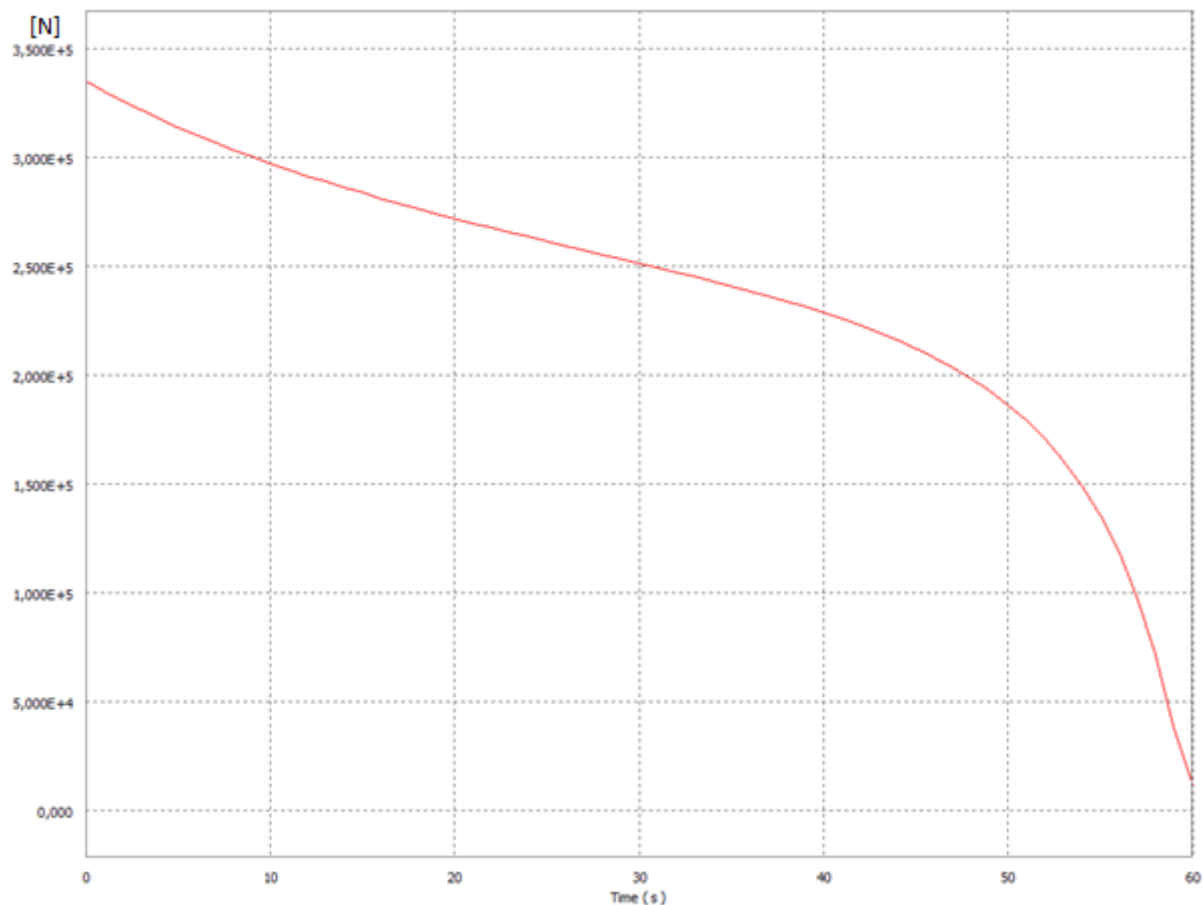


Figure C.11: Diagram illustrates how the lifting force changes as a function of time

C.3 Winch with push rod

This concept is similar to the screw jack with push rod. The electric cylinder is replaced by a winch and several pulleys and these are responsible for reducing the forces involved.

The design uses the sliding push rod to lift the ramp cover, but the lifting mechanism itself is a rig with at least two winches set up in such a way so the force required to lift the ramp cover is dramatically reduced. The reduction is caused by using several pulleys as it can be seen in Figure C.12 below.

The total wire length L_{tot} is a sum of L_{drum} , L_{stroke} and L_{τ} . $L_{drum} = n \cdot 2\pi \cdot R_{drum}$, n is the amount of laps the wire must be wrapped around the drum in order to achieve a higher friction coefficient so the winch will operate properly. $L_{stroke} = Stroke \cdot amount\ of\ reductions$ where the stroke is described by Equation B.3 and $L_{\tau} = \frac{u}{\tan\tau}$. L_{τ} is the minimal length required so the angle τ doesn't exceed the tolerance of $1,5^{\circ}$. This tolerance ensures the wires don't grind each other as they get pulled. All parameters can be found in Figure C.12.

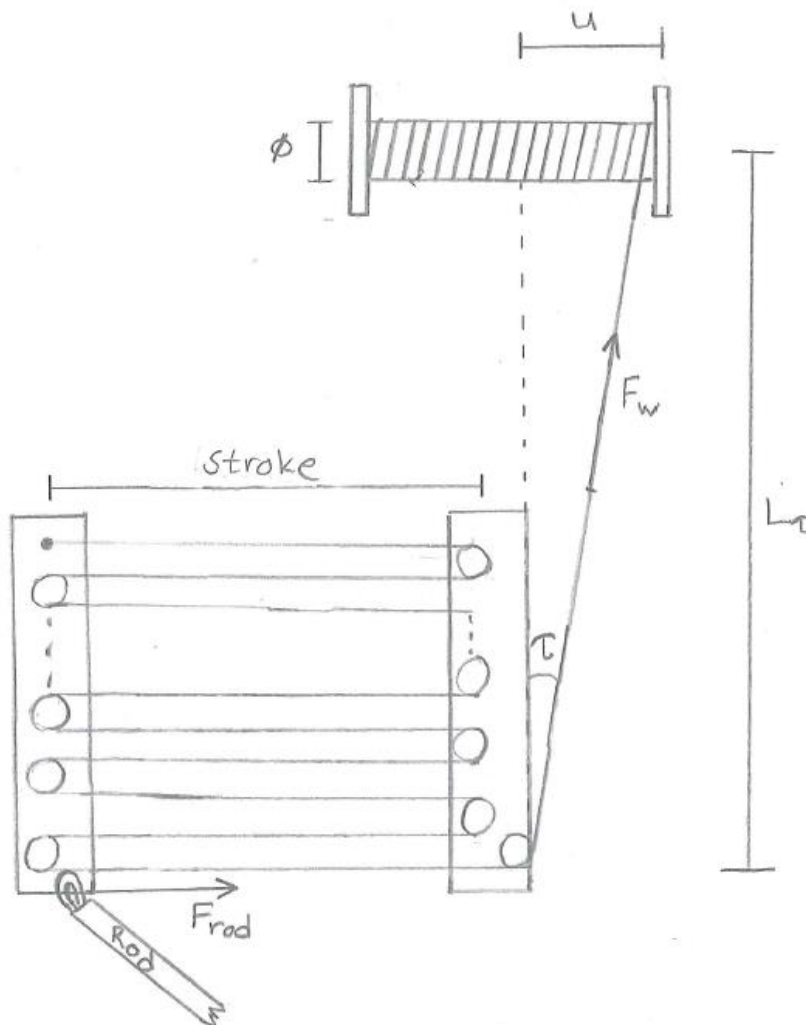


Figure C.12: Representation of the winch mechanism

A disadvantage with using winches is, you can't use them to deliver a pushing force. To overcome this problem some mechanism must be used to initiate the closing operation, for example springs or a mechanical cylinder.

The ramp cover must be able to close even if the boat is leaning 5° (see Figure C.13 below). The forces required to tip the ramp cover are show below:

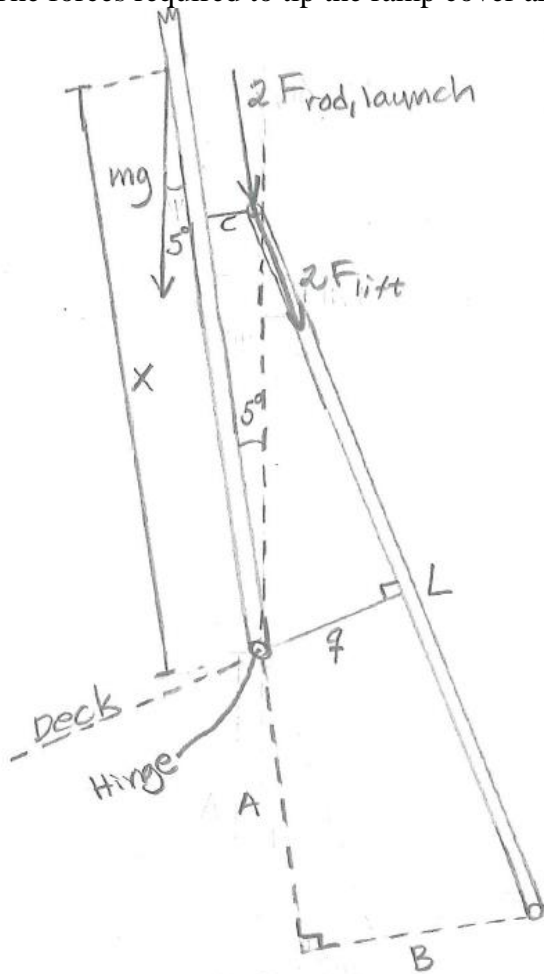


Figure C.13: The ramp cover in its opening position if the boat is leaning 5 degrees

A moment equation around the ramp cover's hinge yielded:

$$2F_{lift} \cdot q(\theta) - mg \cdot x \cdot \sin 5^\circ = 0$$

where q was obtained from the equations under the headline "B.1.1 Calculations to describe the lever q " with $\theta = 90^\circ$.

x is the coordinate describing the position of the center of mass of the ramp cover and m is the mass of the ramp cover.

A vertical force equation results in:

$$F_{lift} = F_{rod} \cdot \cos \phi, \text{ but since } \phi \text{ is very small } F_{lift} \approx F_{rod}$$

$$\therefore F_{rod} \approx \frac{mg \cdot x \cdot \sin 5^\circ}{2 \cdot q(90)}$$

The force required to push the winch rig in order to make the ramp cover tip is a sum of F_{rod} , $F_{winch\ rig}$ and F_w . $F_{winch\ rig}$ is the force required to move the rig with all the pulleys when the ramp cover is leaning 5° (see Figure C.13 above).

$F_{winch\ rig} = m_{winch\ rig} \cdot g \cdot \cos 5^\circ$ where $m_{winch\ rig}$ is the mass of the rig with the pulleys.

F_{w+} is the force required to activate the winch's sensors so the winch will start feeding the cable and this force is defined as $F_{w+} = n \cdot F_w$, n is the amount of times the force is stepped up and F_w is 10% of the nominal lifting force of the winch [8].

Therefore the force required to tip the ramp cover (F_{launch}) is the following sum:

$$F_{launch} = \frac{mg/2 \cdot x \cdot \sin 5^\circ}{q(90)} + m_{winch\ rig} \cdot g \cdot \cos 5^\circ + n \cdot F_w ,$$

F_{launch} is maximal at the beginning of the closing operation when the ship leans 5° but will decline dramatically as this angle moves from 5° towards 0° and after passing 0° the ramp cover's own mass will take over.

C.4 Direct pushing cylinder

This system works in exactly the same way as with a hydraulic cylinder (Figure C.14). The difference is, instead of using a hydraulic cylinder, a mechanical cylinder is used (Figure C.15). The mechanical cylinder can have a worm gear or use screw rollers and can be connected with a drive shaft in order to be driven in parallel if desired.

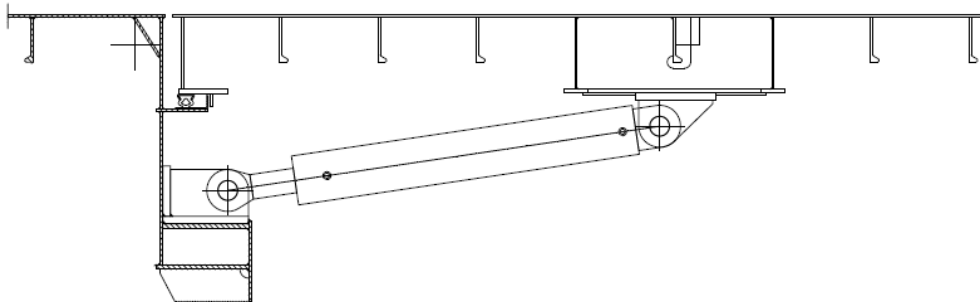


Figure C.14: A cross section view of a hydraulic cylinder



Figure C.15: Mechanical cylinder from Swedrive [4]

One of the downsides of this system is the cost (see Appendix D), since these mechanical cylinders need to be dimensioned for buckling they become large and this is one of the factors that increase their cost. However, this concept is the easiest way to replace the hydraulic cylinder. This is always a possible solution for TTS Marine AB but it is expensive and since it is a finished product there is not that much more analysis required.

Appendix D. Economic references

As mentioned earlier in this report all costs have been estimated by discussing with relevant personnel in the TTS Marine AB office in Gothenburg:

- Henrik Adlersson, about the hydraulic system: the cylinder, the pipes, PLC programmable logic controller (steering system) [9].
- Tobias Ahlberg, about hydraulic design [8].
- Joe Corbett, about piping design [10].

All other costs have been estimated by Henrik Westermark and Peter Adolphsson [2,11].

The mechanical design cost of the current design is set to zero hours because this concept works as the reference concept. The other concepts have been compared to the current design and the extra hours that would be required to design have been documented below.

No consideration will be taken to the cleating (locking) system, this impacts the piping design, reducing it by 50% in all the concepts.

Hydraulics - Current Design			
Design	Hours	SEK/h	Total
Mech. Design	0	500	0
Hydraulic Design	25	880	22000
Piping Design 15%	90	500	45000
Electric design	0	880	
Electrics	Qty	SEK/unit	
Cables	0	70	0
Installation cableing 4 cables 5m/h	0	80	0
Cables brake	0	20	0
electric screw jack	0	55000	0
electric motor 18kW	0	18000	0
PLC+Op. Cab.	1	45000	45000
Steel structure	Qty	SEK/unit	
Wagon steel	0	2500	0
Glide pads	0	200	0
Axel R.F.	0	350	0
	Mass [kg]	SEK/kg	
Guide	0	12	1000
Rod	0	12	0
Hydraulics	Qty	SEK/unit	
Cylinders (160/110)	2	18000	36000
Valve Block	1	27000	27000
	Length [m]	SEK/length	
Pipes (20/16)	80	40,3	3224
	Length [m]	(SEK/2h)*m	
Piping Installation	80	800	64000
Flushing			8000
Add-ons	Qty	SEK/unit	
Vertical lock	2	7500	15000
		Total SEK	266224

*Installation refers to the cable installation and it is 4 cables that need to be set up and they are normally installed at a rate of 5 meters per hour.

*PLC + Operation Cabinet includes motor starter and contactor

Screw jack with push rod			
Design	Hours	SEK/hour	Total
Mech. Design	20	500	10000
Hydraulic Design	0	880	0
Piping Design 5%	30	500	15000
Electric design	0	880	0
Electrics	Length [m]	SEK/m	
Cables	80	70	5600
Installation cableing 4 cables 5m/h	40	80	3200
Cables brake	80	20	1600
	Qty	SEK/unit	
electric screw jack	2	55000	110000
electric motor 18kW	2	18000	36000
PLC+operation cab. (contactor+motor starter)	1	52000	52000
Steel structure	Qty	SEK/unit	
Wagon steel	2	2500	5000
Glide pads	8	200	1600
Axel R.F.	4	350	1400
	Mass [kg]	SEK/kg	
Guide	300	12	4600
Rod	290	12	3480
Hydraulics	Qty	SEK/unit	
Cylinders (160/110)	0	18000	0
Valve Block	0	27000	0
	Length [m]	SEK/length	
Pipes (20/16)	0	40,3	0
	Length [m]	(SEK/2h)*m	
Piping Installation	0	800	0
Flushing	0		
Add-ons	Qty	SEK/unit	
Vertical lock	0	7500	0
		Total SEK	249480

Winch mechanism			
Design	Hours	SEK/h	Total
Mech. Design	60	500	30000
Steel structure	Qty	SEK/unit	
Wagon steel	2	2500	5000
wheel	8	500	4000
Bearings	8		0
Axel R.F.	4	350	1400
pulleys	32	200	6400
	Mass	SEK/kg	
Guide	300	12	4600
Rod	290	12	3480
Pulley house	250	12	3000
Electrics	Qty	SEK/unit	
frequency changer	2	20000	40000
PLC	1	45000	45000
Wunsch	2	35000	70000
	Length [m]	SEK/m	
Cables	80	70	5600
Cables brake	80	20	1600
Installation*	40	80	3200
Wire (8 laps)	50	75	3750
		Total SEK	227030

Infinity link - Screw Jack			
Design	Hours	SEK/h	Total
Mech. Design	30	880	26400
Steel structure	Qty	SEK/unit	
Wagon steel	2	2500	5000
wheel	8	500	4000
Bearings	8		0
Axel R.F.	4	350	1400
pulleys	32	200	6400
	Mass	SEK/kg	
Link arm	320	12	3840
Rod	290	12	3480
Axle	20	35	700
Guide	300	12	3600
Electrics	Qty	SEK/unit	
Screw jack	2	45000	90000
PLC	1	45000	45000
Motor	2	20000	40000
	Length [m]	SEK/m	
Installation*	40	80	3200
Cables	80	70	5600
Cables brake	80	20	1600
		Total SEK	240220

Infinity link - Mech. Cyl.

Design	Hours	SEK/h	Total
Mech. Design	30	880	26400
Steel structure	Qty	SEK/unit	
Wagon steel	2	2500	5000
wheel	8	500	4000
Bearings	8		0
Axel R.F.	4	350	1400
pulleys	32	200	6400
	Mass	SEK/kg	
Link arm	320	12	3840
Rod	290	12	3480
Axle	20	35	700
Guide	300	12	3600
Electrics	Qty	SEK/unit	
Mech. Cyl.	2	100000	200000
PLC	1	45000	45000
	Length	SEK/m	
Installation*	40	80	3200
Cables	80	70	5600
Cables brake	80	20	1600
		Total SEK	310220

Direct pushing cylinder

As mentioned earlier, this cylinder will have to push with a force comparable to about 30 ton but since a 25 ton lifting mechanisms seem to be the largest standard within the market no cost could be estimated for this concept. A mechanical cylinder made for 25 ton without the need to withstand buckling has a roughly estimated cost of 100 000 kr [4], which means a pushing mechanical cylinder made for 30 ton will have a higher cost, making this concept costly.

Appendix E. The rejected solutions

The early rejected solution, the solutions that were never looked into more detail, can be found in this appendix.

E.1 Vertical mechanical cylinder pull

This is a variant of the screw jack with push rod. Here the mechanical cylinder is placed under the ramp cover's hinge as in Figure E.1 and it pulls the push rod which in its turn pushes the ramp cover open.

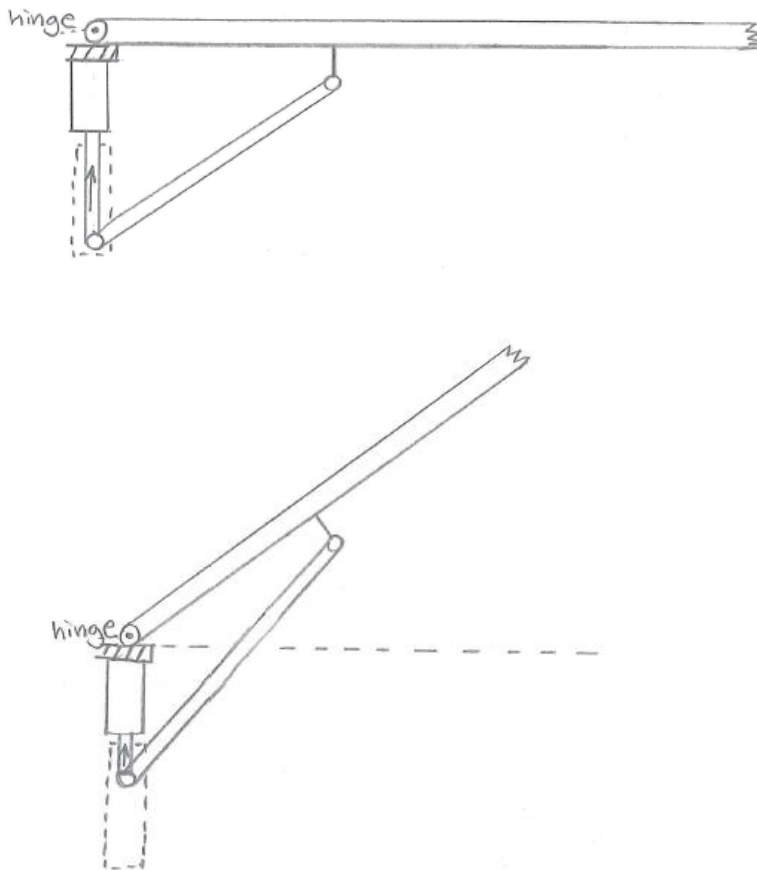


Figure E.1: Describes the lifting mechanism of the vertical mechanical cylinder pull

In this concept the spindle will not need to withstand any buckling force but this concept demands quite a lot of space below the ramp cover, which doesn't fulfill all the requirements.

E.2 Winch ceiling

A winch is placed on the deck above and a wire is lowered and locked onto the ramp cover as far away from the hinge as technically possible (see Figure E.2). The winch hoists the ramp cover open.

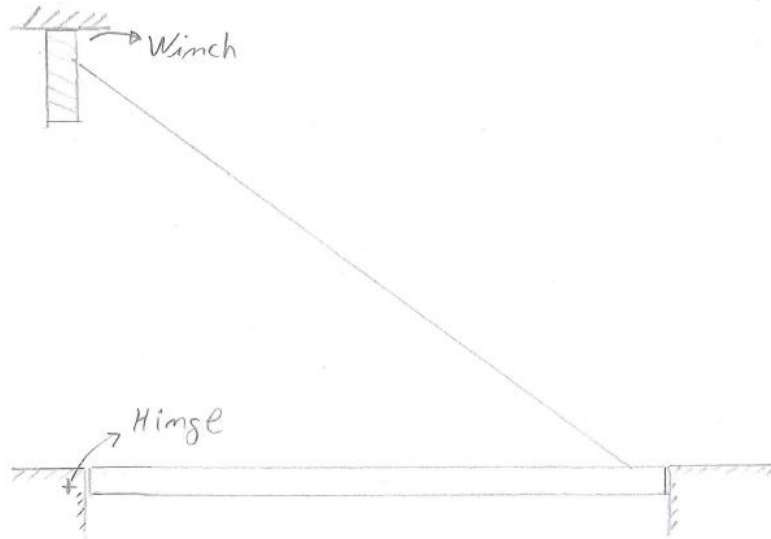


Figure E.2: Lifting mechanism for the concept: Winch ceiling

There must be a mechanism that guides the wire to the right place on the ramp cover if not a person has to do it by hand. The last one is not an option, it would become too complicated and also one of the requirements was that the opening process should be automatic. This concept requires a solution to make the ramp cover close, since the winch cannot push. This system would have utilized a long lever which would have diminished the force required to lift the ramp cover significantly.

E.3 Help cylinder

Extra cylinders are placed on the opposite side of the ramp cover's hinge and these cylinders will be smaller and serve only as assistants to the main cylinders, see Figure E.3.

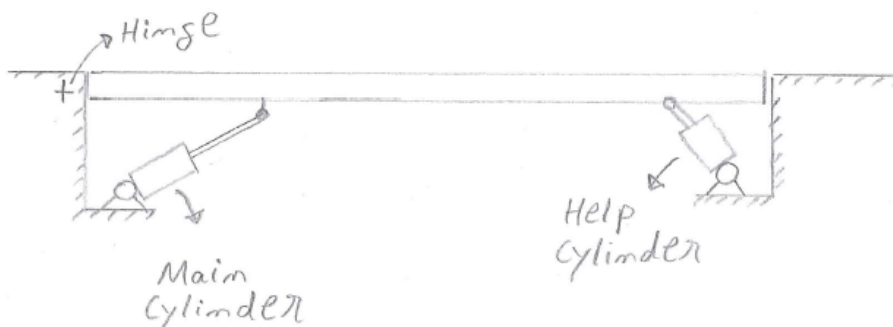


Figure E.3: Lifting mechanism of Help cylinder

The idea of having these help cylinders is to minimize the force on the main cylinder but the help cylinders will need to help the main cylinders for too long to give a significant difference. The calculations from the current design showed that the center of mass of the

ramp doesn't move that much during the first 40-50° of the opening angle, see Equation A.1 and Figure A.2.

E.4 Hinge torque

An electrical motor is connected directly to the ramp cover's hinge, see Figure E.4, and opens the cover by rotating the hinge.

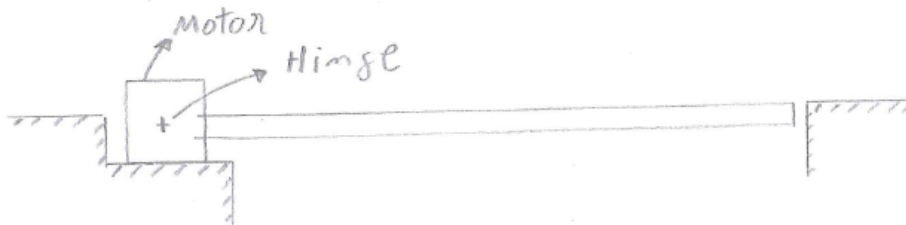


Figure E.4: The opening mechanism of Hinge torque

This method requires large torque and strains the hinge connected to the cover. The strains and the stresses here are going to be very large so in order to make the axle withstand the strain the axle has to be quite large. Even the motor is going to be large and the cost will increase with the size of the motor.

E.5 Rack pinion

This solution is a lot like “hinge torque”, the design is also going to open the cover by turning the hinge, see Figure E.5, but this concept has a rack pinion linked together with a gear at the cover's hinge. When the rack pinion moves in the arrow's direction the gear at the hinge starts to rotate and the cover will open.

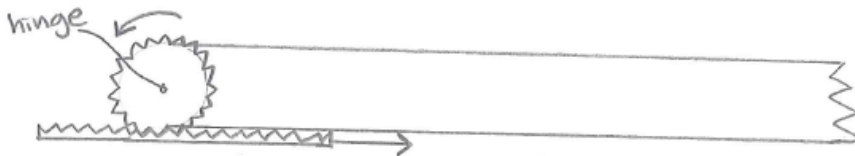


Figure E.5: Opening mechanism of Rack pinion

This concept will also require a large torque and since just one or maybe two cogs are in contact at the same time, the cogs need to cope with large forces. In order for the cogs to manage these forces they need to be quite large and therefore this concept becomes too expensive.